AWARD NUMBER: W81XWH-18-1-0312

TITLE: Biomarkers for predicting response to immune checkpoint blockers

PRINCIPAL INVESTIGATOR: Kiyoshi Ariizumi, PhD

CONTRACTING ORGANIZATION: UT Southwestern Medical Center

REPORT DATE: OCTOBER 2021

TYPE OF REPORT: Final report

PREPARED FOR: U.S. Army Medical Research and Development Command
Fort Detrick, Maryland 21702-5012

REPORT DOCUMENTATION PAGE

Form Approved
OMB No. 0704-0188

1. REPORT DATE	2. REPORT TYPE	3. DATES COVERED
OCTOBER 2021	Final Report	07/01/18 - 06/30/2021

4. TITLE AND SUBTITLE
Biomarkers for predicting response to immune checkpoint blockers

5a. CONTRACT NUMBER
LC170125

5b. GRANT NUMBER
W81XWH-18-1-0312

5c. PROGRAM ELEMENT NUMBER
GRANT12488737

6. AUTHOR(S)
Kiyoshi Ariizumi, PhD

E-Mail:

5d. PROJECT NUMBER

5e. TASK NUMBER

5f. WORK UNIT NUMBER

7. PERFORMING ORGANIZATION NAME(S) AND ADDRESS(ES)
UT Southwestern Medical Center

8. PERFORMING ORGANIZATION REPORT NUMBER

9. SPONSORING / MONITORING AGENCY NAME(S) AND ADDRESS(ES)
U.S. Army Medical Research and Development Command
Fort Detrick, Maryland 21702-5012

10. SPONSOR/MONITOR'S ACRONYM(S)

11. SPONSOR/MONITOR'S REPORT NUMBER(S)

12. DISTRIBUTION / AVAILABILITY STATEMENT
Approved for Public Release; Distribution Unlimited

13. SUPPLEMENTARY NOTES

14. ABSTRACT

Objectives/Hypotheses: We discovered a new immune checkpoint pathway, termed DC-HIL/syndecan-4. DC-HIL receptor is expressed by blood MDSC in NSCLC patients, but very-low to not-at-all by healthy individuals. We found that DC-HIL (but not PDL1) mediates MDSC s T-cell suppressor function -- anti-DC-HIL mAb neutralizes this function, converting cancer-bearing mice from resistant to responsive recipients of anti-PD1/PDL1 mAb. Moreover, the soluble DC-HIL receptor (sDC-HIL) is a strong promoter of lung metastasis. Thus exponential expansion of DC-HIL+ MDSC may account for the resistance of NSCLC patients to anti-PD1/PDL1 mAb. Not only will we prove this hypothesis, but we will also probe the mechanisms underlying treatment resistance and identify markers that can sort responders from non-responders.
Specific Aims: Aim 1: Determine whether DC-HIL expression prognosticates responsiveness to anti-PD1/PDL1 mAb treatment in lung cancer patients. We will assess the influence of DC-HIL and PDL1 by measuring: their relative expression on blood MDSC and tumor cells, blood sDC-HIL levels, and their ability to suppress T-cell activation. NSCLC patients will be treated with anti-PD1/PDL1 mAb, screened and assessed prior to treatment and at predetermined intervals during treatment and up to 2 years. Aim 2: Identify MDSC genes that underlie responsiveness/resistance to anti-PD1/PDL1 therapy. Because tumor-derived factors transform MDSC into a phenotype that potently suppresses T-cell function, thereby countering therapeutic effects of immune checkpoint blockers, we hypothesize that MDSC possess genes whose expression determines responsiveness/resistance of NSCLC patients to anti-PD1/PDL1 treatment. MDSC gene expression profiles will be compared between responders vs. non-responders to anti-PD1/PDL1 therapy.
Study Design: In Aim 1, blood samples will be collected from NSCLC patients who enroll for anti-PD1/PDL1 mAb treatment at different time points (including pretreatment), in which FACS analysis will be used to determine frequency of DC-HIL+ MDSC in total PBMC, fluctuation of DC-HIL expression during the treatment, sDC-HIL in the plasma, and MDSC ability to suppress autologous T cells. Tumor biopsies before treatment will be examined for expression of PDL1 vs. DC-HIL. Correlation of DC-HIL expression with non-responders (or responders) will be statistically analyzed. In Aim2, RNA isolated from purified MDSC will be subjected to whole genome expression analysis using RNA-Seq.
Impact: Identification of DC-HIL or other MDSC genes as a prognosticator of response to anti-PD1/PDL1 therapy will greatly improve management of NSCLC patients, providing guidance regarding choice of therapy with attendant savings in time and money. These results will lead to the hypothesis that blood level of DC-HIL+ MDSC (or related indexes) serve as useful biomarker(s) for predicting responsiveness/resistance to anti-PD1/PDL1 therapy. Our results will also provide insight into the relative benefits of monotherapy vs. combination therapy) of anti-DC-HIL and anti-PD1/PDL1 mAb in NSSCLC patients.
Military Relevance: NSCLC is the leading cause of metastasis in the U.S. and a common cause of morbidity and mortality among Military Service members, Veterans, and their families. Our outcomes should improve survival rate of those members and their family and save the budget for military-associated medical treatment.

15. SUBJECT TERMS
DC-HIL biomarker for immune cancer therapy

16. SECURITY CLASSIFICATION OF:			17. LIMITATION OF ABSTRACT	18. NUMBER OF PAGES	19a. NAME OF RESPONSIBLE PERSON
a. REPORT	b. ABSTRACT	c. THIS PAGE			USAMRDC
Unclassified	Unclassified	Unclassified	Unclassified	23	19b. TELEPHONE NUMBER *(include area code)*

Standard Form 298 (Rev. 8-98)
Prescribed by ANSI Std. Z39.18

TABLE OF CONTENTS

1. INTRODUCTION:

Cancer remains a leading cause of mortality among Americans and the lung is the primary site of origin for these deaths. Among available treatments for metastatic lung cancer, immune checkpoint blockers are associated with the best survival rates, with anti-PD1/PDL1 monoclonal antibodies (mAb). Yet, even this therapeutic advance benefits only a minority (<20%) of metastatic lung cancer patients. Furthermore, there are no good markers for sorting which patients will or will not respond to treatment. Our purpose is to identify biomarkers that reliably prognosticate responsiveness (vs. resistance) of metastatic lung cancer patients to anti-PD1/PDL1 mAb.

2. KEYWORDS:

Biomarker
DC-HIL
Immune checkpoint inhibitors
Immunotherapy
Myeloid-derived suppressor cells
Non-small cell lung carcinoma
PD-1/PD-L1
Prediction of response
Resistance

3. ACCOMPLISHMENTS:

- What were the major goals of the project?

  (1) Blood levels of DC-HIL$^+$MDSC before treatment discriminate between responders and non-responders to anti-PD1/PDL1 mAb.

  Period: 2 years
  Percentage of completion: 90%

  (2) Fluctuation of DC-HIL expression.

  Period: 2 years
  Percentage of completion: 90%

  (3) Blood sDC-HIL level

  Period: 2 years
  Percentage of completion: 100%

  (4) Recovery of T-cell function

  Period: 1 year
  Percentage of completion: 100%

  (5) Tumor-DC-HIL and -PDL1 expression

  Period: 6 months
  Percentage of completion: 70%

  (6) Identify MDSC genes that underlie responsiveness/resistance to anti-PD1/PDL1 therapy.

  Period: 1 year
  Percentage of completion: 20%

- What was accomplished under these goals?

  1) Major activities

  Identifying new patients; recruiting them, taking blood samples from patients every 3-6 weeks after immunotherapy; determining marker expression; collecting and organizing treatment history of patients;

evaluating patients' response to immunotherapy; performing statistical analysis; and molecular wroks with RNA isolated from myeloid-derived suppressor cells (MDSC).

2) Specific objectives:

a) Determine whether DC-HIL expression prognosticates responsiveness to anti-PD1/PDL1 mAb treatment in lung cancer patients

b) Identify MDSC genes that underlie responsiveness/resistance to anti-PD1/PDL1 therapy

3) Significant results or key outcomes, including major findings, developments, or conclusions (both positive and negative);

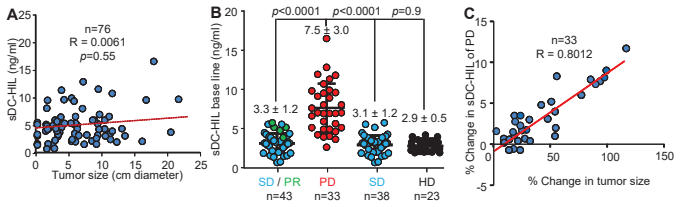

Fig. 1. Correlation of baseline blood sDC-HIL levels and response of NSCLC patients to ICI therapy. A, Blood sDC-HIL levels of NSCLC patients (n=76) at baseline are plotted against initial tumor size (sum of tumor cm diameter). **B,** NSCLC patients were evaluated for response to ICI at Week ~12 after the first cycle and sorted into non-responders (PD) and responders (SD and PR). Blood sDC-HIL levels (mean ± SD) at baseline are compared between these 2 cohorts. SD and healthy donors (HD) are separately compared to each other. P values are shown using Mann-Whitney *U* test. **C,** % change in sDC-HIL levels of PD patients (n=33) is plotted against % change in tumor size between Weeks 0 and 6. Pearson Correlation Coefficient R = 0.8012 with p=0.00001.

Hypotheses that were proven in this funding period:

1. Baseline blood sDC-HIL levels associate with poor response of non-small cell lung carcinoma (NSCLC) to anti-PD1/PD-L1 immunotherapy. Blood samples were taken from metastatic NSCLC patients just prior to immune checkpoint inhibitor (ICI) therapy and determined by ELISA for sDC-HIL levels. To evaluate the predictive value of this baseline sDC-HIL level, we compared with tumor size before treatment (baseline) **(Fig. 1A)**. There was no significant correlation between these two parameters. Patients were sorted based on 6 week response to ICI into responders (who showed stable disease (PD) or partial response (PR)) and non-responders (who developed progressive diseases or PD). Evaluation was executed using Response evaluation criteria in solid tumors (RECIST) 2.0 criteria. Baseline sDC-HIL level in non-responders was significantly higher than that in responders, which was similar to healthy donors **(Fig. 1B)**. Moreover, changes in sDC-HIL levels in the period of 6 weeks after onset of treatment also correlated with changes in tumor size **(Fig. 1C)**. These data indicate that blood sDC-HIL level may be a biomarker to predict cancer response to ICI therapy.

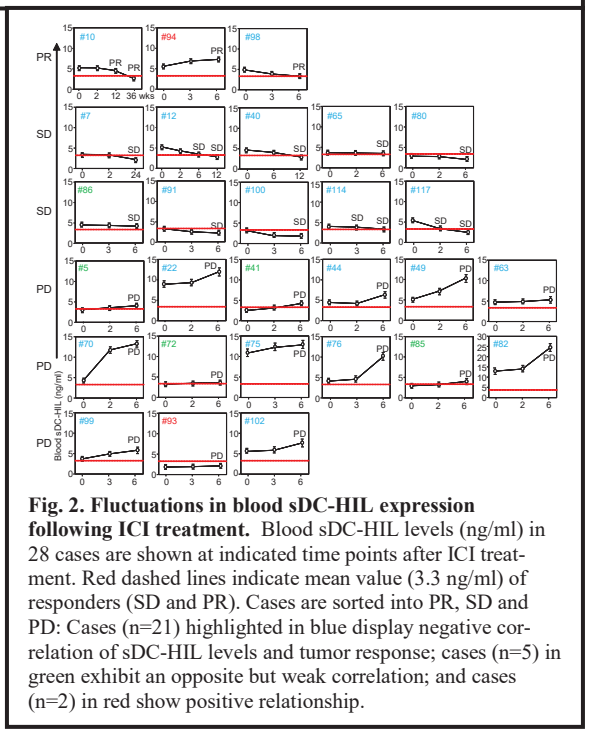

Fig. 2. Fluctuations in blood sDC-HIL expression following ICI treatment. Blood sDC-HIL levels (ng/ml) in 28 cases are shown at indicated time points after ICI treatment. Red dashed lines indicate mean value (3.3 ng/ml) of responders (SD and PR). Cases are sorted into PR, SD and PD: Cases (n=21) highlighted in blue display negative correlation of sDC-HIL levels and tumor response; cases (n=5) in green exhibit an opposite but weak correlation; and cases (n=2) in red show positive relationship.

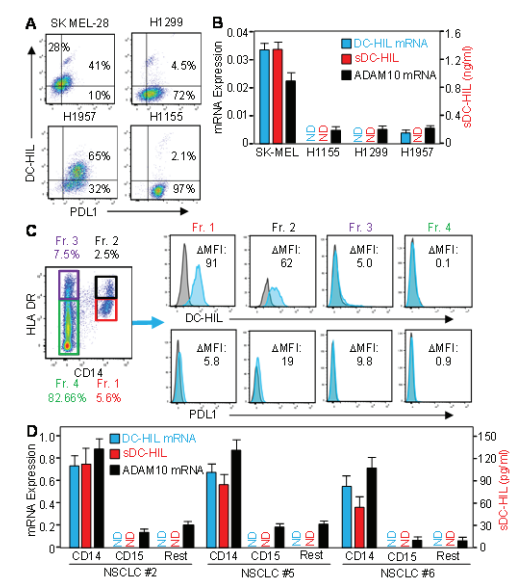

Fig. 3. Expression of DC-HIL by lung cancer cells vs. PBMC from NSCLC patients. A, 3 NSCLC cell lines and SK-MEL-28 melanoma (as reference) were examined by FACS for expression of DC-HIL vs. PDL1 receptors and shown by % positivity. **B,** These cells were assayed by qRT-PCR for mRNA expression of DC-HIL (blue bars) and ADAM10 (black bars) relative to GAPDH and determined for secretion of sDC-HIL (red bars with the right y-axis) in the culture. ND, not determined. **C,** PBMC of NSCLC patients (n=5) were fluorescently stained with Ab to HLA-DR and CD14, and sorted into 4 fractions; Fr. 1 (HLA-DR$^{no/lo}$ CD14^{+} cells); Fr. 2 (HLA-DR$^{med/hi}$ CD14^{+}); Fr. 3 (HLA-DR$^{med/hi}$ CD14^{neg}); and Fr. 4 (HLA-DR$^{no/lo}$ CD14^{neg}). Each fraction was assayed for expression of DC-HIL and PDL1 receptors. **D,** PBMC from blood of patients (n=3) were sorted into 3 fractions (CD14^{+}, CD15^{+} and others) and quantified for DC-HIL and ADAM10 mRNA and sDC-HIL protein.

2. sDC-HIL level increased as tumors were growing.
We examined fluctuations over time duration of ICI therapy. We collected blood samples at every 2-3 weeks (n=28) and addressed whether the level changes depending on cancer response. Twenty

one out of 28 cases tested (78%) exhibited sDC-HIL levels to increase as tumors are growing (PD phenotype) or decreasing as tumors are shrinking. Five cases showed weak correlation with tumor response and 2 cases did an opposite correlation (high or low levels in patients with PR and PD, respectively). Thus, blood sDC-HIL levels fluctuate in real-time according to tumor response, indicating that sDC-HIL is a marker to show the present status of immune suppression in patients.

3. MDSC are sDC-HIL-producers, but not cancer cells. We next addressed what cells secrete the most sDC-HIL in patients; cancer cells or leukocytes? NSCLC cell lines were assayed for expression of DC-HIL receptor (vs. PD-L1), mRNA for DC-HIL and ADAM10 genes (the latter is a sheddase that cleaves DC-HIL receptor), and sDC-HIL secretion in the cell culture. One out of 3 lines expressed high-levels of DC-HIL on the cell surface, but no secretion of sDC-HIL nor expression of ADAM10 mRNA **(Fig. 3A** and **3B)**. For blood circulating leukocytes, PBMCs of patients were fluorescently stained with anti-HLA-DR and anti-CD14 Ab and sorted by FACS into 4 fractions; (1) $CD14^{+}HLA\text{-}DR^{no/lo}$ (MDSC); (2) $CD14^{+}HLA\text{-}DR^{+}$ (containing antigen-presenting cells); (3) $CD14^{neg}HLA\text{-}DR^{hi}$ (mainly B cells); and (4) $CD14^{neg}HLA\text{-}DR^{neg}$ (containing T cells). Fr.1 and Fr.2 expressed substantial levels of DC-HIL (but not PD-L1). $CD14^{+}$ cells (including MDSC) were purified and tested for sDC-HIL secretion, and we found $CD14^{+}$ cells to be producers of sDC-HIL **(Fig. 3C** and **3D)**.

Hypotheses that were not proven in this funding period:

1. MDSC expansion did not correlate with poor response to ICI therapy. We recruited separately metastatic NSCLC patients and similarly assayed for % of monocytic or granulocytic MDSC among total PBMCs and also DC-HIL expression in each MDSC subpopulation. These variables were compared between responders and non-responders **(Fig. 4)**. For all variables (monocytic and granulocytic subpopulation; and DC-HIL cell surface expression), we were unable to see significant differences in between responders and non-responders. Thus, sDC-HIL level can be a biomarker to predict response, whereas % of DC-HIL receptor-expressing MDSC in blood may not have a predictive value for tumor response. This result seems contradictory to the data that MDSC is the major source of sDC-HIL, suggesting the existence of sDC-HIL-secretors other than MDSC.

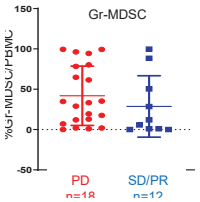

Fig. 4. Comparison of MDSC expansion in blood of no-responders vs. responders to ICI therapy. In separate recruitment (n=30 NSCLC), blood samples prior to treatment with anti-PD1/PDL1 Ab (ICIs) were determined by FACS for frequency (%) of monocytic $CD14^{+}HLA\text{-}DR^{no/lo}$ **(A)** or % of granulocytic $CD15^{+}HLA\text{-}DR^{no/lo}$ MDSC **(B)** and % $DC\text{-}HIL^{+}$ MDSC subpopulation in total PBMCs. Patients were sorted into responders (PR or SD, n=12) and non-responders (PD, n=18), based on tumor response evaluated at 6 weeks-follow up. There was no significant (ns) correlation of MDSC expansion marker and poor tumor response to ICI.

2. Technical difficulties in determination of whole genome transcriptome (Aim 2). We proposed to determine transcriptome of monocytic MDSC isolated from blood of responders and non-responders and determine signature genes that are expressed differentially in these patient groups. For this assay, a series of sequential steps are needed, which include collecting 30 ml of peripheral blood from a patient (n=5), purifying PBMCs, FACS-analyzing % MDSC, isolating MDSC, extracting and purifying mRNA, amplifying RNA signals by PCR, and subjected to RNA-Seq analysis. We had several difficulties, (1) only few patients agreed to provide 30 ml volume (1-5 ml for most cases); (2) a huge variation in yield of MDSC,

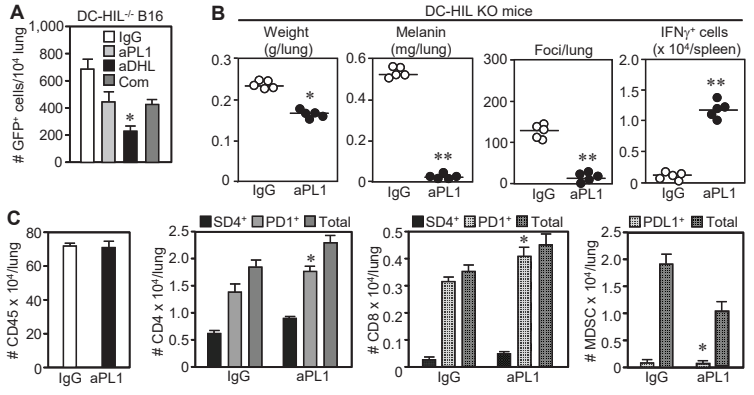

Fig. 5. Host (but not tumor) DC-HIL determines tumor response to ICI therapy. **A,** Mice bearing lung-metastatic GFP^{+} $DC\text{-}HIL^{-/-}$B16 cells were similarly treated with control IgG (IgG), anti-PDL1 (aPL1), anti-DC-HIL (aDHL) or combination (Com), and tumor growth was quantified by number of GFP^{+} cells among 10,000 lung cells. **B and C,** $DC\text{-}HIL^{-/-}$ mice with B16 lung mets were treated with control IgG or anti-PDL1 mAb. Lung metastasis was quantified for indicated indices (**B**) and lung cells were prepared and determined by flow-cytometry for number of $CD45^{+}$ leukocytes, $CD4^{+}$ or $CD8^{+}$ T-cells ($SD4^{+}$, $PD1^{+}$ subset or total cells) per total lung (**C**).

due to small volume, unknown impurities that contaminate in MDSC fraction, which block subsequent PCR amplification; and (3) very low yield of mRNA per cell, 2-5-fold lower than other leukocytes and lymphocytes. We have to develop or apply cutting-edge techniques (e.g., single cell RNA-Seq) that allow reliable whole genome RNA-Seq analysis with trace amounts of cells.

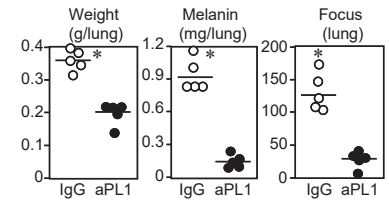

Fig. 6. Non-hematopoietic DC-HIL is dispensable for resistance to ICI therapy. BM chimeric mice with transplantation of BM cells of DC-HIL$^{-/-}$ mice were injected *i.v.* with B16 cells and treated with IgG or anti-PDL1 mAb, followed by scoring metastasis in lung; the weight; total melanin content; and foci number.

Other achievements:

1. DC-HIL expression in host hematopoietic cells determines tumor response to anti-PDL1 treatment in mouse tumor model. We addressed whether DC-HIL expression determines tumor response to ICIs.

1.a. Tumor DC-HIL expression is irrelevant to tumor response:

Among tumor lines, B16 melanoma is unique in expressing DC-HIL. We used this model to examine whether tumor-DC-HIL expression accounts for resistance to anti-PDL1 therapy. We generated DC-HIL-knocked out (DC-HIL$^{-/-}$) B16 cells that do not express DC-HIL but retain high expression of PDL1. Using this cell line, we examined influence of tumor-DC-HIL to anti-PDL1 response **(Fig. 5A)**. DC-HIL$^{-/-}$ B16 cells showed as a poor response to anti-PDL1 as did the parental cells, indicating that tumor-DC-HIL has no influence to this resistance. We then addressed whether host DC-HIL affects anti-PDL1 response **(Fig. 5B)**. DC-HIL$^{-/-}$ mice bearing B16 lung mets were treated with anti-PDL1 or control IgG. Anti-PDL1 treatment led to a remarkable decrease in all metastasis indices in DC-HIL$^{-/-}$ mice; including lung weight (0.23 vs. 0.18 g), melanin content (0.53 vs. 0.03 mg) and number of foci (127 vs. 14), with a 10-fold increase in IFN-γ response. Although there was no difference in CD45^{+} tumor-infiltrating leukocytes (TIL) number between anti-PDL1 and control treatments, anti-PDL1 mAb increased total CD4 and CD8 T-cells and their SD4+ and PD1+ subsets, while decreasing total MDSC in the lung **(Fig. 5C)**.

1.b. Non-hematopoietic cells have no contribution to the resistance:

Because DC-HIL is also expressed by non-hematopoietic cells, we dissected influence of hematopoietic cell- vs. non-hematopoietic cell-derived DC-HIL to anti-PDL1 response. We generated bone marrow (BM)-chimeric mice, in which hematopoietic cells are originated from transplanted BM cells of DC-HIL$^{-/-}$ mice. Deletion of DC-HIL gene from hematopoietic cells (while non-hematopoietic DC-HIL expression remains) failed to reverse the high response to anti-PDL1 **(Fig. 6)**, indicating that DC-HIL on non-hematopoietic cells is dispensable for B16 melanoma resistance to anti-PDL1 treatment.

1.c. Both DC-HIL receptor-expressing MDSC and sDC-HIL are resistance factors for ICI response.:

Because melanoma-bearing hosts express DC-HIL as the receptor on MDSC and sDC-HIL, we addressed which molecular form is more important in regulating tumor responsiveness to anti-PDL1 mAb. For the impact of DC-HIL receptor, we examined whether adoptive transfer of DC-HIL^{+} MDSC into DC-HIL$^{-/-}$ mice bearing B16 lung mets reverses anti-PDL1 tumor response **(Fig. 7A).** As control, DC-HIL^{neg} MDSC were also transferred into the host. Reproducibly, anti-PDL1 inhibited growth of B16 lung mets almost completely in DC-HIL$^{-/-}$ mice. This antitumor activity was diminished markedly by infusion of DC-HIL^{+} MDSC, whereas injection of DC-HIL^{neg} MDSC had no effect.

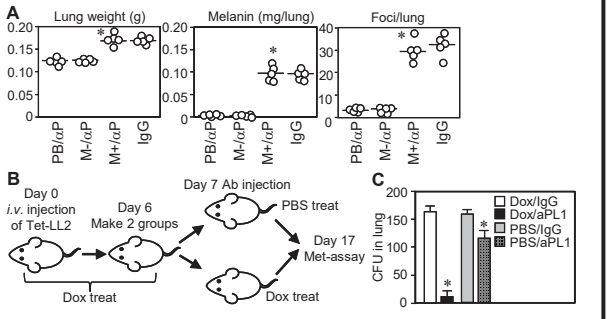

Fig. 7. Both DC-HIL+ MDSC and sDC-HIL regulate ICI response. A, DC-HIL$^{-/-}$ mice with B16 lung mets were given *i.v.* injection of PBS (PB), DC-HIL^{neg} (M-) or DC-HIL^{+}MDSC (M+) and then treated with anti-PDL1 mAb (αP). IgG group was treated just with control IgG. After 5 injections, mice were quantified for metastasis indices. **F** and **G,** LL2-neo cells with Tet-Off-controlled sDC-HIL gene were injected *i.v.* into mice treated with Dox. On day 6, all mice were sorted into 2 groups, treated with Dox or PBS, followed by *i.p.* injection of anti-PDL1 mAb or control IgG (**F**). On day 17, mice were quantified for metastasis by counting CFU of G418-resistant colonies and expressed as CFU in 1 x 10^{6} lung cells (**G**). *p<0.0001 compared to control.

For sDC-HIL, we used LL2 lung cancer cells (which do not express DC-HIL) transfected with Tet-Off-controlled sDC-HIL gene **(Fig. 7B)**. Immediately after *i.v.* injection of the LL2 transfectants, mice were given doxycycline (Dox, which shuts off DC-HIL expression) for 6 days, and

then sorted into 2 groups; one was continued with Dox and the other was discontinued. These groups were also treated with anti-PDL1 or control IgG and scored for metastasis indices on day 17. sDC-HIL remained very low through day 6, but quickly increased to 8.4-9.6 ng/ml after Dox discontinuation, and low sDC-HIL levels (1-1.4 ng/ml) were maintained in Dox-continued group that exhibited very high response to anti-PDL1 mAb compared to IgG-treated mice **(Fig. 7C)**. By contrast, Dox-discontinued group (sDC-HIL expressed) had markedly reduced antitumor activity. This reduced response was associated with increased total MDSC or DC-HIL$^+$ subset of lung mets. Thus, both DC-HIL$^+$ MDSC and sDC-HIL converted tumor cells from an anti-PDL1-responsive to resistant tumor. However, this conclusion may be not true for metastatic NSCLC patients. We will investigate the contradiction.

- **What opportunities for training and professional development has the project provided?**
  Nothing to Report.

- **How were the results disseminated to communities of interest?**
  We published most of data shown above in the scientific journal "*Clinical Cancer Research*".

- **What do you plan to do during the next reporting period to accomplish the goals?**
  This is final report.

4. IMPACT:

- **What was the impact on the development of the principal discipline(s) of the project?**
  Our studies documented the possibility that blood DC-HIL serves as a biomarker that predict which patients with metastatic lung cancer will respond (vs. not respond) to the currently best immunotherapy anti-PD1/PDL1 mAb.

- **What was the impact on other disciplines?**
  Nothing to Report

- **What was the impact on technology transfer?**
  Our finding of blood sDC-HIL to be a promising prognosticator of response to immunotherapy in the most common type "non-small cell lung carcinoma (NSCLC) will greatly improve management of NSCLC patients, providing guidance regarding choice of therapy with attendant savings in time and money. This finding also will provide a clue to establish "Precious Cancer Immunotherapy". Another impact is that we revealed the future possibility that DC-HIL is a pharmacological target for augmenting the efficacy of ICI therapy by combining with anti-PDL1 because DC-HIL is the potent resistant factor. Creation of effective humanized mAb against human DC-HIL may lead to the development of new cancer therapeutic drugs.

- **What was the impact on society beyond science and technology?**
  Lung cancer is the leading cause of metastasis in the U.S. and a common cause of morbidity and mortality among Military Service members, Veterans, and their families. Our findings should improve survival rates of afflicted patients and lead to savings in medical expenses and patients' precious time.

5. CHANGES/PROBLEMS:

- **Changes in approach and reasons for change**
  We had several significant difficulties to conduct this project. First, delay in start of patient recruitment, due to delay of filling IRB for this study. Second, suddenly in August 2019, monotherapy with anti-PD1/PDL1 mAb became no longer available for treatment of NSCLC patients (which is our target disease), except for patients with high expression levels of PDL1 on tumors. However, such patients in clinic are very rare (<5% of total NSCLC patients). Instead, this immunotherapy is advised to combine

with chemotherapy. Thus, we had to change the patient recruitment strategy. Third, since March 16, UT Southwestern medical center has discontinued Tissue Core Services that provide us with blood samples of NSCLC patients, due to the COVID-19 pandemic in the Texas State. These difficulties have impacted significantly on the progress of our research. As of July 1, 2020, we requested one year-extension with no extra cost. Almost one year later, the Tissue Core Service Facility at UT Southwestern medical center restarted collecting human clinical samples (March 1, 2021). Since then, we resumed this project to collect patients' blood samples and analyze immunological phenotype and functional properties, but only 3 new cases were added to our studies. Instead, we have studied the mutual interactions between DC-HIL and PDL1 in regulation of cancer immunity using mouse model.

- **Actual or anticipated problems or delays and actions or plans to resolve them**
  Refer to the above.

- **Changes that had a significant impact on expenditures**
  Refer to the above. We had technical difficulties in Aim 2.

- **Significant changes in use or care of human subjects, vertebrate animals, biohazards, and/or select agents.**
  Refer to the above.

- **Significant changes in use or care of human subjects**
  Refer to the above.

- **Significant changes in use or care of vertebrate animals.**
  Nothing to report

- **Significant changes in use of biohazards and/or select agents**
  Nothing to report.

6. PRODUCTS:

- **Publications, conference papers, and presentations**
  Chung J-S, Ramani V, Kobayashi M, Fattah F, Popat V, Zhang S, Cruz PD Jr., Gerber DE, **Ariizumi K**. DC-HIL/Gpnmb is a negative regulator of tumor response to immune checkpoint inhibitors. *Clin Cancer Res* 15; 1449-1459. 2020. PMID: 31822499

- **Website(s) or other Internet site(s)**
  Nothing to report.

- **Technologies or techniques**
  Nothing to report.

- **Inventions, patent applications, and/or licenses**
  Nothing to report.

- **Other Products**
  Nothing to report.

7. PARTICIPANTS & OTHER COLLABORATING ORGANIZATIONS

Name:	*Kiyoshi Ariizumi*

Project Role:	*PI*
Researcher Identifier (e.g. ORCID ID):	*0000-0002-6630-4440*
Nearest person month worked:	*3.6*
Contribution to Project:	*Dr. Ariizumi has supervised all members in this project, made a publication and prepared the final report.*
Funding Support:	*VA Merit Award and NIHRO1*

Name:	*Jin-Sung Chung*
Project Role:	*Fellow*
Researcher Identifier (e.g. ORCID ID):	*0000-0001-9450-5939*
Nearest person month worked:	*4.8*
Contribution to Project:	*Dr. Chung has performed some of human studies and provided other fellows with technical advices.*
Funding Support:	*VA Merit Award.*

Name:	*Vijay Ramani*
Project Role:	*Fellow*
Researcher Identifier (e.g. ORCID ID):	*0000-0001-5449-0242*
Nearest person month worked:	*9*
Contribution to Project:	*Dr. Ramani has executed some experiments in human studies and most of animal studies. .*
Funding Support:	*VA Merit Award*

Name:	*Masato Kobayashi*
Project Role:	*Fellow*
Researcher Identifier (e.g. ORCID ID):	*0000-0001-7717-8948*
Nearest person month worked:	*6*
Contribution to Project:	*Dr. Kobayashi has performed most of human studies.*
Funding Support:	*Dermatology department support.*

Name:	*Irene Dougherty*
Project Role:	*Other roles*
Researcher Identifier (e.g. ORCID ID):	*Not available*
Nearest person month worked:	*2.4*
Contribution to Project:	*Ms. Dougherty has prepared and ensured IRB approval and maintained the laboratory.*
Funding Support:	*Dermatology departmental support*

Name:	*Yvonne Gloria-McCutchen*
Project Role:	*Other roles*
Researcher Identifier (e.g. ORCID ID):	*Not available*
Nearest person month worked:	*1.2*
Contribution to Project:	*Ms. Gloria-McCutchen has coordinated patients' visit schedule and blood drawing.*
Funding Support:	*Oncology departmental support*

- **Has there been a change in the active other support of the PD/PI(s) or senior/key personnel since the last reporting period?**
  Nothing to report

- **What other organizations were involved as partners?**
  Nothing to report.

8. SPECIAL REPORTING REQUIREMENTS

Nothing to report.

9. APPENDICES:

Attached Pdf is the published paper in *Clinical Cancer research* journal.

Published OnlineFirst December 10, 2019; DOI: 10.1158/1078-0432.CCR-19-2360

DC-HIL/Gpnmb Is a Negative Regulator of Tumor Response to Immune Checkpoint Inhibitors

Jin-Sung Chung[1], Vijay Ramani[1], Masato Kobayashi[1], Farjana Fattah[2], Vinita Popat[2], Song Zhang[3], Ponciano D. Cruz Jr[1], David E. Gerber[2], and Kiyoshi Ariizumi[1]

ABSTRACT

Purpose: Immune checkpoint inhibitors (ICI) benefit only a minority of treated patients with cancer. Identification of biomarkers distinguishing responders and nonresponders will improve management of patients with cancer. Because the DC-HIL checkpoint differs from the PD1 pathway in expression and inhibitory mechanisms, we examined whether DC-HIL expression regulates ICI responsiveness.

Experimental Design: Plasma samples were collected from patients with advanced non–small cell lung carcinoma (NSCLC) ($n = 76$) at baseline and/or follow-up after ICI monotherapy. Blood-soluble DC-HIL (sDC-HIL) was determined and analyzed for correlation with the early tumor response. To study the mechanisms, we measured effect of anti-DC-HIL versus anti-PDL1 mAb on growth of mouse tumor cells in experimentally metastatic lung. Influence of DC-HIL to anti-PDL1 treatment was assessed by changes in tumor response after deletion of host-*DC-HIL* gene, injection of DC-HIL–expressing myeloid-derived suppressor cells (MDSC), or induction of sDC-HIL expression.

Results: Nonresponders expressed significantly higher levels of baseline sDC-HIL levels than responders. Among patients ($n = 28$) for fluctuation with time, nonresponders (14/15 cases) showed increasing or persistently elevated levels. Responders (12/13) had decreasing or persistently low levels. Among various tumors, B16 melanoma exhibited resistance to anti-PDL1 but responded to anti-DC-HIL mAb. Using B16 melanoma and LL2 lung cancer, we showed that deletion of host-derived DC-HIL expression converted the resistant tumor to one responsive to anti-PDL1 mAb. The responsive state was reversed by infusion of DC-HIL$^+$MDSC or induction of sDC-HIL expression.

Conclusions: sDC-HIL in the blood and probably DC-HIL receptor expressed by MDSC play an important role in regulating response to ICI in advanced NSCLC.

Introduction

Antigen-specific T cells are activated by a net-stimulatory balance arising from competition between costimulatory and coinhibitory signals transduced by binding of receptors and ligands expressed on the surface of T cells and antigen-presenting cells or suppressor cells (1). The coinhibitory molecules, also termed "immune checkpoints," include CTLA4/CD80 and PD1/PDL1 (2).

Many cancers that overexpress immune checkpoint molecules exude a net-inhibitory balance that can dampen natural anticancer immunity (3). Immune checkpoint inhibitors (ICI) were developed to circumvent this problem, blocking delivery of coinhibitory signals and thus amplifying antitumor responses (4). Among these ICI, anti-PD1/PDL1 mAb (e.g., nivolumab, pembrolizumab, and atezolizumab) have produced improved objective response rates, including 10% to 20% in cases of non–small cell lung carcinoma (NSCLC; ref. 5), 12% to 28% for melanoma (6, 7), approximately 43% for bladder cancer (8), and 10% to 20% for renal cell cancer (9). Despite these unprecedented benefits, the majority of metastatic cancers have initial resistance to ICI therapy (10). Thus, the development of reliable biomarkers that identify patients who will not respond to ICI therapy before treatment or even during the course of treatment could bring a great benefit to cancer treatment.

We identified a new immune checkpoint pathway comprising the DC-HIL [also known as Gpnmb (11)] receptor and its T-cell ligand, heparan sulfate-attached syndecan-4 (SD4; refs. 12, 13). DC-HIL is expressed constitutively by some cancer cells (including melanoma, breast and lung cancers; refs. 14, 15) and can be induced on myeloid-derived suppressor cells (MDSC) that proliferate exponentially in blood of patients with various malignancies (16). Patients with metastatic NSCLC produced 0.3% DC-HIL-expressing MDSC among peripheral blood mononuclear cells (PBMC), which was significantly higher than healthy controls (0.05%). DC-HIL–expressing cells release the soluble form (sDC-HIL) by cleaving off the extracellular domain by ADAM10 proteinase (17). Both DC-HIL and PDL1 receptors are expressed on tumor cells and mediate cancer-induced immunosuppression (18), but their interactions with suppressor cells differ: PDL1 mediates regulatory T-cell (Treg) function but is less important to MDSC (12, 16). In contrast, DC-HIL is the critical mediator of MDSC function and insignificant to Treg (12). Moreover, their respective T-cell ligands (SD4 and PD1) reside in disparate loci and signal independently of each other: PD1 associates with the CD3ζ chain of the T-cell receptor complex (19), whereas SD4 is separate from this complex (20). Therefore, DC-HIL and PDL1 pathways regulate T-cell response by distinct mechanisms.

To evaluate the hypothesis that DC-HIL counteracts the augmented T-cell response by ICI treatment, we examined whether patients with

[1]Department of Dermatology, the University of Texas Southwestern Medical Center, and Dermatology Section (Medical Service), North Texas Veterans Affairs Medical Center, Dallas, Texas. [2]Department of Hematology Oncology, The University of Texas Southwestern Medical Center, Dallas, Texas. [3]Department of Population Data Sciences, The University of Texas Southwestern Medical Center, Dallas, Texas.

Note: Supplementary data for this article are available at Clinical Cancer Research Online (http://clincancerres.aacrjournals.org/).

Current address for M. Kobayashi: Departments of Veterinary Clinical Pathology and Veterinary Science, Nippon Veterinary and Life Science University, Tokyo, Japan.

Corresponding Author: Kiyoshi Ariizumi, The University of Texas Southwestern Medical Center, NL8.108A, 5323 Harry Hines Blvd, Dallas, TX 75390. Phone: 214-648-2860; Fax: 214-648-5554; E-mail: kiyoshi.ariizumi@utsouthwestern.edu

Clin Cancer Res 2020;26:1449–59

doi: 10.1158/1078-0432.CCR-19-2360

Published OnlineFirst December 10, 2019; DOI: 10.1158/1078-0432.CCR-19-2360

Translational Relevance

Despite unprecedented improvement in survival of patients with cancer treated with immune checkpoint inhibitors (ICI), most patients are resistant to this therapy for reasons that remain elusive. Thus, the identification of reliable biomarkers predicting the responders to ICI therapy could bring a great benefit to cancer treatment. Among ICI-treated patients with advanced non–small cell lung carcinoma, elevated blood sDC-HIL levels at the baseline were associated with disease progression and poor outcomes. In animal studies, DC-HIL levels, expressed as the receptor on myeloid-derived suppressor cells and/or its soluble form (sDC-HIL) in blood, correlated directly with resistance to anti-PDL1 treatment. These findings indicate DC-HIL's negative influence on current ICI therapy, highlighting its potential as a blood biomarker to predict treatment responsiveness and clinical benefit.

advanced NSCLC express sDC-HIL in the blood and whether the high levels associate with poor response to ICI therapy. We found high blood sDC-HIL levels to correlate strongly with resistance to ICI therapy in patients with advanced NSCLC. To study mechanisms by which DC-HIL attenuates response to ICI, we searched mouse tumor lines resistant to anti-PDL1 mAb but sensitive to anti-DC-HIL mAb. Among four tumor lines examined, B16 melanoma was distinct in its contrasting responses to the two treatments, such that cancer regression followed anti-DC-HIL mAb infusion, whereas only a marginal effect was achieved by anti-PDL1 treatment (18, 21). However, similar experiments using mice devoid of the DC-HIL gene (DC-HIL KO) resulted in regression of melanoma in response to anti-PDL1 mAb, indicating that resistance to anti-PDL1 treatment in wild-type mice involved expression of host DC-HIL. These findings were also confirmed with mouse LL2 lung cancer. Our studies suggest that host DC-HIL expression may be a biomarker to predict tumor response of patients with advanced NSCLC to ICI therapy.

Materials and Methods

Patients with NSCLC

Patients with advanced NSCLC ($n = 76$, Supplementary Table S1) who had ICI treatment between 2015 and 2017 at Harold C. Simons Comprehensive Cancer Center at The University of Texas Southwestern Medical Center, Dallas, TX, were included in this study (22). Patients were treated with standard of care ICI monotherapy (atezolizumab, nivolumab, or pembrolizumab) every 2 to 3 weeks (23, 24). Response to treatment was determined at every 6 to 12 weeks by RECIST version 1.1 (25). Each patient provided informed consent before enrollment. The Institutional Review Board of UT Southwestern approved this study (STU-082015-53). Peripheral blood samples were collected from all patients before treatment (week 0) and some patients provided samples at 2 and 6 weeks posttreatment. Plasma was obtained by centrifugation (at 2,000 g for 10 minutes) and supernatant collected and stored at −80°C. The study was conducted in accordance with the amended Declaration of Helsinki and the International Conference on Harmonization Guidelines.

Reagents, animals, and cell culture

Leukocyte marker Ab and antimouse PDL1 mAb (10F.9G2) were purchased from eBioscience and Bio-X-Cell, respectively. We generated UTX103 rabbit antimouse DC-HIL mAb (14) and the chimeric UTX103 IgG (UTX-m16) was constructed by replacing the C-region of UTX103 rabbit IgG with that of mouse IgG_1. These Abs were produced by transient transfection of suspension cultures with the IgG genes using ExpiCHO systems in serum-free media (Thermo Fisher Scientific) and purified by Protein A-agarose (Invitrogen). Purified preparations comprise very low endotoxin level (<0.05 EU/mL), determined by Pierce Chromogenic Endotoxin Quant Kit. Female C57BL/6 mice (∼8-week-old) and pmel-1 TCR transgenic mice were purchased from Harlan Breeders and The Jackson Laboratory, respectively. Animals were housed in the pathogen-free facility of the Institutional Animal Care Use Center of UT Southwestern Medical Center. All animal protocols were approved by the Center. Mouse tumor lines were purchased from the American Type Culture Collection, Old Town Manassas, VA, and maintained in DMEM supplemented with 10% FCS. Human NSCLC cells were obtained from Hamon Center for Therapeutic Oncology Research, UT Southwestern, Dallas, TX.

For leukocyte isolation and culture, PBMC from blood (∼15 mL) of patients with NSCLC ($n = 3$) were divided into two parts: one was stained with fluorescently labeled anti-HLA-DR and anti-CD14 and analyzed by flow cytometry for receptor expression; the other was treated sequentially with anti-CD14 Ab-coated magnetic beads (for monocytes) and anti-CD15-beads (granulocytes). The rest contained B and T cells. These fractions were cultured for 2 days with GM-CSF (100 ng/mL) or IL2 (20 unit/mL) and assayed for mRNA expression and sDC-HIL levels in culture supernatant.

sDC-HIL ELISA

An aliquot (100 μL) of 5× PBS-diluted plasma samples was applied to ELISA wells in triplicate (human GPNMB R&D Systems). For measuring mouse sDC-HIL levels in blood and culture supernatant, 1:100-diluted or undiluted samples were used. To allow reliable and unbiased method comparison, all tests were done in a single-blind manner by an independent laboratory technician.

DC-HIL-deleted B16 melanoma

pGuide-it-ZsGreen vector (Clontech Laboratories Inc) containing DC-HIL-targeted gRNA (CCGGCCGAAGACCAGCCACGTAAT) and CAS9 was transfected into B16 melanoma cells with Lipofectamine LTX with PLUS Reagent (Life Technologies) in Opti-MEM I (Life Technologies). After transfection, DC-HIL-deleted B16 cells were enriched by cell sorting using BD FACS Aria (BD Biosciences) and confirmed by immunoblotting for null DC-HIL expression.

mAb treatment

Tumor cells were harvested from the growing cultures by ethylene diamine tetra-acetic acid (EDTA), washed extensively with PBS, and injected intravenously into mice [$(2–5) \times 10^5$ cells/mouse] via tail vein. Six days postinjection, all mice were given intraperitoneal injection of mAb (200 μg/mouse) every 2, 3, or 4 days at the total of six injections. Two days after the last injection (day 18), mice were scored for metastatic indices, lung weight, number of foci, and melanin content in the tissue (18). For other tumor cells, GFP-transfected cells were injected intravenously into mice, and lung-metastatic tumor cells were counted by flow cytometry: Lung was perfused with PBS and single-cell suspension isolated by digesting with collagenase/dispase (Roche), collagenase type I/IV, and DNAase I (Sigma-Aldrich) for 90 minutes at 37°C and passed through a 40-μm membrane. For experiments measuring survival rate, all mice were injected intravenously with B16 cells (1×10^5 cells/mouse) and day 6 they were randomly sorted into four groups ($n = 10$) and given different mAb every 2 days until

Published OnlineFirst December 10, 2019; DOI: 10.1158/1078-0432.CCR-19-2360

day 16; thereafter, schedule was changed to longer intervals; every 3 days until day 28; and every week until day 60.

Analysis of tumor microenvironment

All mice were anesthetized, blood drawn from heart, and serum prepared using BD Microtainer. After sacrificing mice, single-cell suspensions [(1–5) × 10^5 cells/reaction] from lung were prepared and fluorescently stained with marker Ab (1–10 μg/mL) to each leukocyte subpopulations, including CD45, CD4, CD8 T cells and their $SD4^+$ or $PD1^+$ subset, and $CD11b^+Gr1^+$ MDSC and their DC-HIL^+ or $PDL1^+$ subsets. After fluorescently labeling with secondary Ab (1 μg/mL), stained cells were analyzed by FACS Verse (BD Biosciences).

Adoptive cell transfer

On day 5 postintravenous injection of B16 cells (2 × 10^5 cells/mouse) into DC-$HIL^{-/-}$ mice, mice were randomly sorted into four groups ($n = 5$) and given intravenous injection of PBS or $CD11b^+Gr1^+$ MDSC (1 × 10^6 cells/mouse) purified from spleen cells of WT or DC-$HIL^{-/-}$ mice bearing subcutaneous B16 melanoma (2 weeks after subcutaneous implantation; ref. 26). $CD11b^+Gr1^+$ fraction from WT mice contained 40% to 50% DC-HIL^+ cells, and that from KO mice had no such cells. On day 6, all mice were treated with anti-PDL1 or control IgG every 2 days.

Tet-off system

Previously, we established LL2 cell line transfected with a vector driving expression of sDC-HIL-V5 under the control of Tet-off system (27). All mice were given 2 mg/mL doxycycline (Dox)-water from day 3 to day 6. Day 0, all mice were injected intravenously with Tet-Off-sDC-HIL-V5-LL2 cells (2 × 10^5 cells/mouse) and day 6 randomly sorted into 2 groups: one group was continuously supplied with Dox (2 μg/mouse intraperitoneal injection every 5 days) and the other discontinued (PBS injection). Since day 7, mice were treated with intraperitoneal injection of anti-PDL1 or control IgG every 2 days ($n = 5$). On day 17 (2 days after the last injection), lung was scored for metastasis indices. Growth of TetOff-sDC-HIL-LL2 cells in lung was measured by clonogenic assays: Total lung cells were seeded in a DMEM-complete media with 600 μg/mL G418 (Sigma-Aldrich). After 10 days in culture, colonies were fixed, stained with crystal violet, and counted. Tumor growth was quantified by colony-forming units (CFU) in total lung cells (lung-CFU).

In vitro assays

To assess gp100-specific T-cell response in mAb-treated mice, spleen cells were prepared and seeded onto ELISPOT wells at varying cell densities with gp100 peptide (5 μg/mL) for 2 days. The IFNγ-producing cells were counted using ELISPOT assay (eBioscience). For Ag-nonspecific response, spleen cells were cultured for 3 days with anti-CD3/CD28 mAb (each 1 μg/mL) and Brefeldin A (Invitrogen), followed by surface staining of CD4 or CD8 and intracellular staining of IFNγ.

Quantitative PCR

This PCR was performed with primers for DC-HIL, ADAM10, or GAPDH (13, 28). mRNA expression in each sample was expressed as the expression level relative to *GAPDH* gene, which was quantitated using the comparative Ct method and the formula 2-ΔΔCT.

Statistical analysis

Mann–Whitney *U* test or Student *t* test was used for comparison. Survival rate and association were evaluated by log rank (Mantel–Cox test) and Pearson's correlation coefficient, respectively. Slope of sDC-HIL levels was analyzed using a mixed-effects model. A $P \leq 0.05$ was considered significant.

Results

Blood sDC-HIL levels are associated with poor response to ICI in advanced NSCLC

We chose NSCLC because of the high prevalence and high expression of DC-HIL by NSCLC cells and circulating MDSC (29). We asked whether patients with NSCLC produce sDC-HIL in the blood. Recruited patients ($n = 76$ and the demographics are summarized in Supplementary Table S1) were measured for tumor size before ICI treatment (6, 24) and evaluated for response to treatment at weeks 6 to 12 (25). Plasma samples were collected at week 0. Blood sDC-HIL was detected at pretreatment (week 0, ≤25 ng/mL) and the levels did not correlate with baseline tumor size (**Fig. 1A**). We then examined

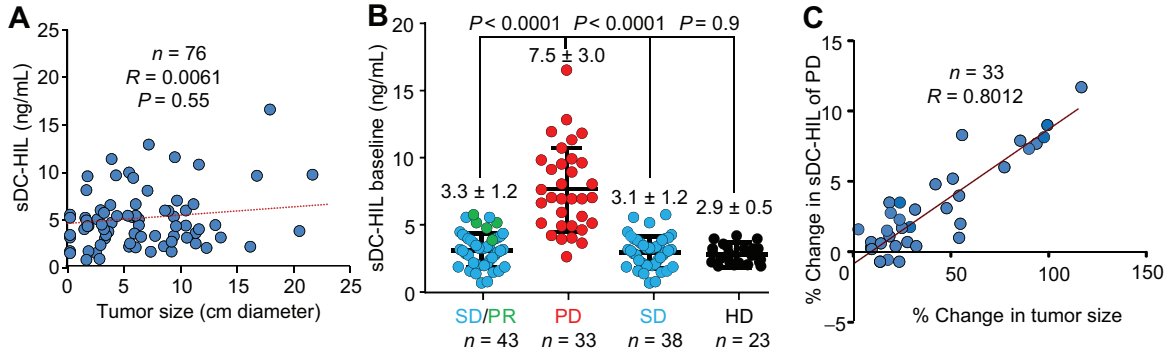

Figure 1.

Correlation of baseline blood sDC-HIL levels and response of patients with advanced NSCLC to ICI immunotherapy. **A,** Blood sDC-HIL levels of patients with NSCLC ($n = 76$) at baseline are plotted against initial tumor size (sum of tumor cm diameter). **B,** Patients with NSCLC were evaluated for response to ICI at week approximately 12 after the first cycle and sorted into nonresponders (PD) and responders (SD and PR). Blood sDC-HIL levels (mean ± SD) at baseline are compared between these two cohorts. The SD and healthy donors (HD) are separately compared with each other. *P* values are shown using Mann–Whitney *U* test. **C,** Percent change in sDC-HIL levels of PD patients ($n = 33$) is plotted against percent change in tumor size between weeks 0 and 6. Pearson correlation coefficient $R = 0.8012$ with $P = 0.00001$.

Published OnlineFirst December 10, 2019; DOI: 10.1158/1078-0432.CCR-19-2360

correlation of baseline sDC-HIL levels and tumor response (**Fig. 1B**), characterizing cases as having progressive disease (PD, $n = 33$), stable disease (SD, $n = 38$), or partial response (PR, $n = 5$) at the first evaluation. Responders (SD and PR) displayed blood sDC-HIL levels (3.3 ng/mL ± 1.2) that are not different from healthy donors (2.9 ± 0.5, $P = 0.9$). In contrast, nonresponders (PD) had significantly higher sDC-HIL levels ($P < 0.0001$ by Mann–Whitney U test) at the baseline. The extent of variation in sDC-HIL levels is similar to that of serum vascular endothelial growth factor, a marker associated with poor outcomes to chemotherapy (30). Among nonresponders, the percent change in sDC-HIL levels within the first 6 weeks after treatment correlated significantly with percent change in tumor size (**Fig. 1C**, $P < 0.00001$).

We also examined fluctuations in sDC-HIL during treatment (**Fig. 2**). In 28 cases for which sDC-HIL levels were available for more than three time points (weeks 0, 2, and 6), we analyzed individual kinetics. Among nonresponders, 14 of 15 cases showed increasing or persistently elevated levels (>3.3 ng/mL, the median of SD/PR groups), whereas one case had low levels at all the time (<3.3 ng/mL). For responders, 12 of 13 cases had decreasing or persistently low levels, with 1 PR patient 94 who showed increasing levels. We then focused on patients ($n = 13$) plotted in the zone of 4 to 6 ng/mL sDC-HIL overlapping between SD/PR and PD groups (**Fig. 1B**). Partial response patients 10 and 98 expressed 5.1 ng/mL sDC-HIL at baseline, which was higher than 3.3 ng/mL. This measure gradually fell at later time points, during which time the treatment response was characterized as PR. Patient 70 (representative of 6 patients) had a baseline measure of 4.3 ng/mL that rose to 11 of 13 ng/mL at weeks 2 and 6; this case's treatment response was judged as PD. In the case of patient 117 (representative of 5 patients), the baseline value of 5.8 ng/mL went down to 3.3 and 2.3 ng/mL and this treatment response was SD. We tested for significant differences in slope among the three groups using a mixed-effects model. The estimated slopes and their 95% confidence intervals (CIs) are as follows: PD: slope = 0.468, 95% CI: 0.273–0.662. PR: slope = −0.145, 95% CI: −0.579 to 0.289. SD: slope = −0.203, 95% CI: −0.441 to 0.035. There was significant difference in slope between SD and PD ($P = 0.001$). There was no significant change in sDC-HIL levels of healthy donors in 2 weeks (Supplementary Table S2). These

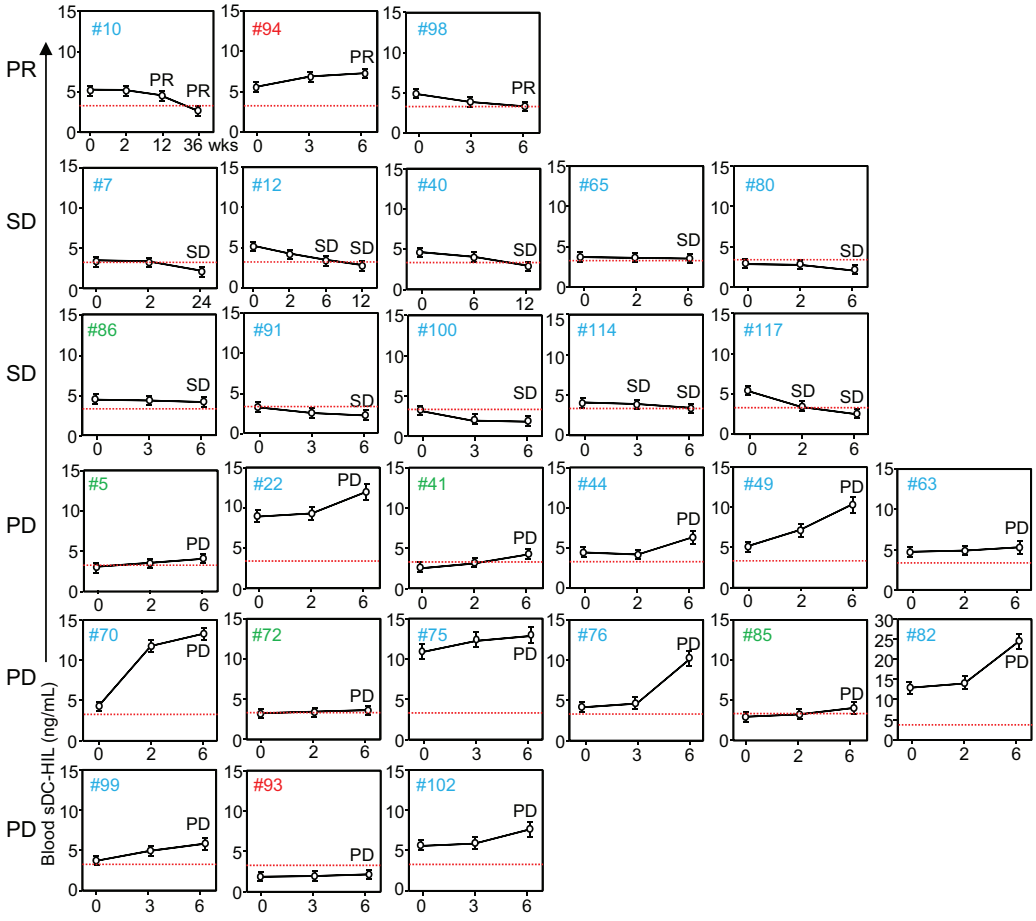

Figure 2.

Fluctuations in blood sDC-HIL expression following ICI treatment. Blood sDC-HIL levels (ng/mL) in 28 cases are shown at indicated time points after ICI treatment. Red dashed lines indicate mean value (3.3 ng/mL) of responders (SD and PR). Cases are sorted into PR, SD, and PD: Cases ($n = 21$) highlighted in blue display negative correlation of sDC-HIL levels and tumor response; cases ($n = 5$) in green exhibit an opposite but weak correlation; and cases ($n = 2$) in red show positive relationship.

Published OnlineFirst December 10, 2019; DOI: 10.1158/1078-0432.CCR-19-2360

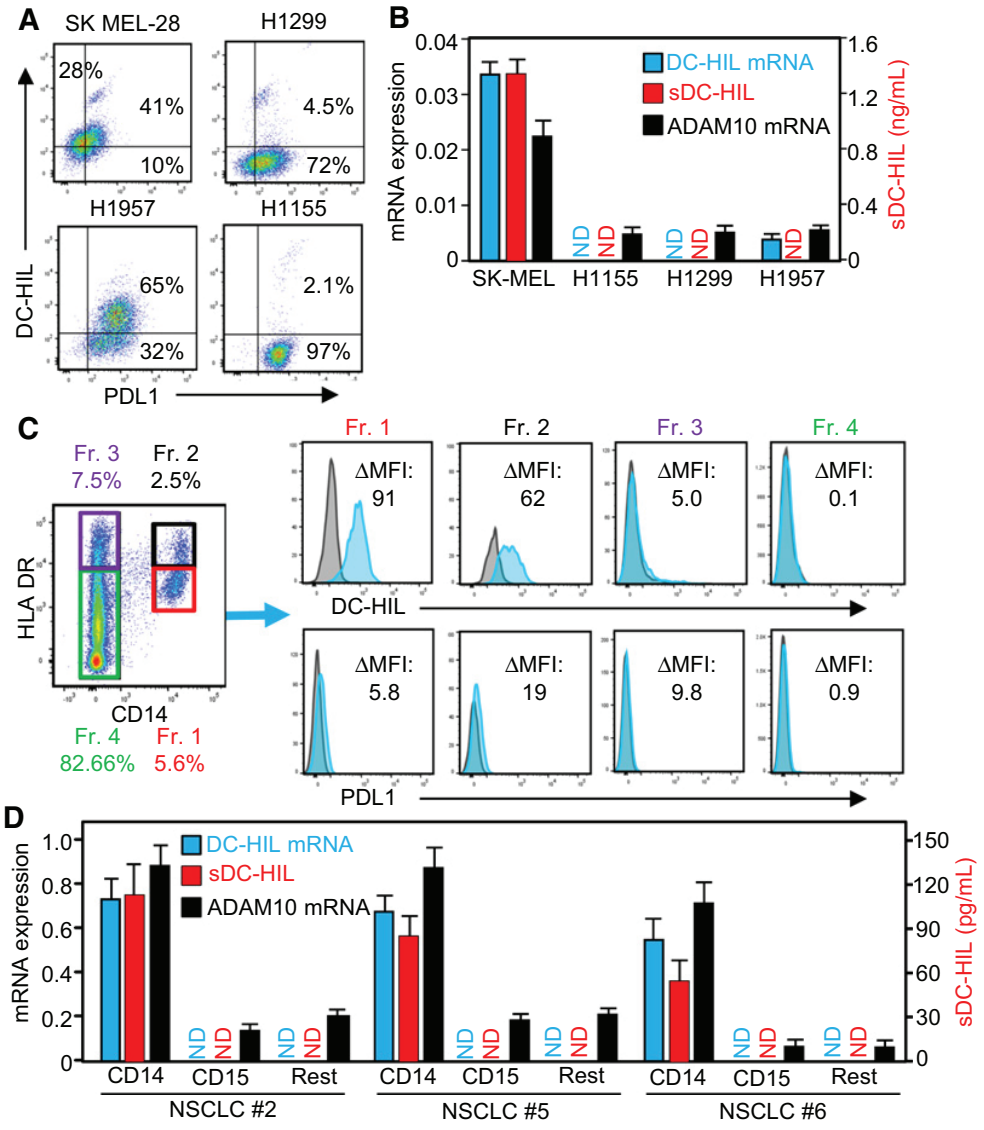

Figure 3.

Expression of DC-HIL by lung cancer cells versus PBMCs isolated from patients with metastatic NSCLC. **A,** Three NSCLC cell lines and SK-MEL-28 melanoma (as reference) were examined by flow cytometry for expression of DC-HIL versus PDL1 receptors. Expression is shown by percent positivity. **B,** These tumor cells were assayed by qRT-PCR for mRNA expression of DC-HIL (blue bars) and ADAM10 (black bars) relative to GAPDH and determined for secretion of sDC-HIL (red bars with the right *y*-axis) in the culture. ND means not determined. **C,** PBMCs of patients with metastatic NSCLC were fluorescently stained with Ab to HLA-DR and CD14 and sorted into four fractions; Fr. 1 (HLA-DR$^{no/lo}$ CD14^{+} cells); Fr. 2 (HLA-DR$^{med/hi}$ CD14^{+}); Fr. 3 (HLA-DR$^{med/hi}$ CD14^{neg}); and Fr. 4 (HLA-DR$^{no/lo}$ CD14^{neg}). Each fraction was determined for expression of DC-HIL and PDL1 receptors. Data shown are representative of 5 patients with NSCLC. **D,** PBMCs from blood of patients with NSCLC ($n = 3$) were sorted into three fractions (CD14^{+}, CD15^{+}, and others) and quantified for DC-HIL and ADAM10 mRNA and sDC-HIL protein.

cases illustrate fluctuations in blood sDC-HIL levels during the treatment, with considerable variation in magnitude and direction of the changes.

Monocytes are the likely producers of sDC-HIL

We probed for which cell types as likely producers of sDC-HIL in patients with NSCLC (**Fig. 3**). To examine DC-HIL expression on tumor cells, we used three NSCLC lines established from cancer biopsies. Among these lines, only H1957 NSCLC line expressed DC-HIL on the cell surface; it was greater than SK-MEL-28 melanoma cell line (**Fig. 3A**) but lower levels of DC-HIL mRNA (**Fig. 3B**). In contrast, all cells expressed PDL1 on the surface constitutively. Despite high levels of surface expression, H1957 line did not produce sDC-HIL in the culture supernatant even when the cell expressed ADAM10 mRNA. For leukocytes, PBMC from patients with NSCLC ($n = 3$) were fluorescently stained with anti-HLA-DR and anti-CD14 Ab

Published OnlineFirst December 10, 2019; DOI: 10.1158/1078-0432.CCR-19-2360

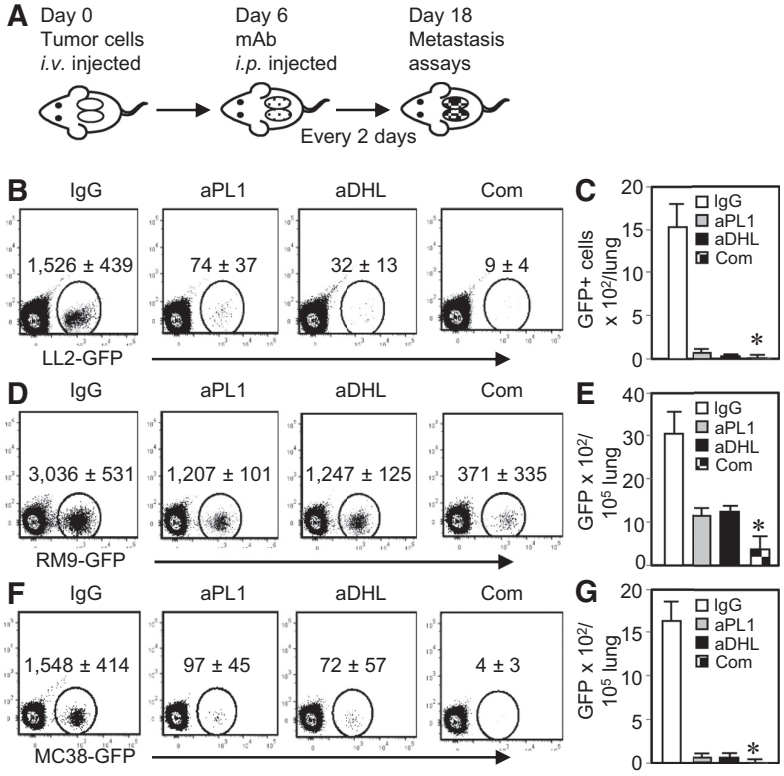

Figure 4.

Combination treatment of anti-DC-HIL and anti-PDL1 mAb produces synergistic antitumor effect on growth of tumors other than B16 melanoma. **A,** Mice were injected intravenously with LL2-GFP lung (**B** and **C**), RM9-GFP prostate (**D** and **E**), or MC38-GFP colon (**F** and **G**) tumor cells and treated with control IgG, anti-PDL1 (aPL1), anti-DC-HIL (aDHL), or combined mAb (Com). On day 18, mice were determined by flow cytometry for number of GFP^+ tumor cells among 10^6 lung cells (**B, D,** and **F**) and data summarized in graphs (**C, E,** and **G**). $^*P < 0.01$ compared between aDHL- and Comb-treated groups. Data shown are representative of at least two independent experiments.

and sorted into four fractions; Fr. 1 (HLA-$DR^{no/lo}$ $CD14^+$ cells); Fr. 2 (HLA-$DR^{med/hi}$ $CD14^+$); Fr. 3 (HLA-$DR^{med/hi}$ $CD14^{neg}$); and Fr. 4 (HLA-$DR^{no/lo}$ $CD14^{neg}$). Each fraction was assayed for DC-HIL and PDL1 expression (**Fig. 3C**). Among these fractions, HLA-$DR^{no/lo}$ MDSC and HLA-$DR^{med/hi}$ $CD14^+$ cells expressed highest levels of DC-HIL (ΔMFI: 91 and 62, respectively), with no expression in the other fractions. We then examined sDC-HIL production by these leukocytes. Because monocytic MDSC are a minuscule fraction, PBMC were sorted into $CD14^+$ monocytes, $CD15^+$ granulocytes, and the other ($CD14^{neg}$ $CD15^{neg}$, which contain B and T cells). DC-HIL mRNA was highest in CD14 monocytes, with no expression by CD15 granular cells (which contain granulocytic MDSC) nor by other leukocytes (**Fig. 3D**). DC-HIL^+ cells also expressed ADAM10 mRNA and secreted sDC-HIL into culture (54–113 pg/mL). Thus, CD14 monocytes, but not tumor cells nor granulocytes, may be the primary source of sDC-HIL.

Among four different tumor lines, lung metastases of B16 melanoma exhibited resistance to anti-PDL1 treatment

To study mechanisms of how DC-HIL attenuates beneficial effect of ICI therapy, we searched mouse tumor lines for the model that exhibits ICI resistance. To measure antitumor activity of anti-PDL1 mAb, we employed experimental metastasis that is the simplest and ideal model because tumor cells are accurately quantified and the target of therapies is often the endpoint of metastasis (31).

We first examined the effects of ICI on pre-established lung mets of LL2 lung cancer. Syngeneic mice were infused intravenously with GFP-transfected LL2 lung cancer cells (that do not express DC-HIL); 6 days later, all mice were treated with anti-DC-HIL, anti-PDL1 mAb alone, or in combination (200 μg/mouse) injected intraperitoneally (six injections total at intervals of 2, 3 or 4 days; **Fig. 4A**). Mice treated with control IgG yielded 1,526 ± 439 GFP^+ LL2 cells per 10^6 lung cells. This index was reduced by anti-PDL1 mAb to 74 ± 37 cells and by anti-DC-HIL to 32 ± 13 cells ($P = 0.08$ vs. anti-PDL1; **Fig. 4B** and **C**). Combined treatment did even better (9 ± 4 cells, $P = 0.01$ vs. anti-DC-HIL). Monotherapy and combined treatment similarly increased CD4 and CD8 T cells in tumor-infiltrating lymphocytes (TIL; including $SD4^+$, $PD1^+$, and $IFN\gamma^+$ subsets; Supplementary Table S3). Interestingly, the same treatment led to reductions in % CD4 (but not % CD8) Treg and % MDSC in TIL. These MDSC expressed DC-HIL but not PDL1 (Supplementary Fig. S1A). We also examined RM9 prostate cancer and noted similar results (**Fig. 4D** and **E**): both mAb individually inhibited growth of RM9 lung mets, and combined treatment achieved better results ($P = 0.01$ to anti-DC-HIL), including reduced $CD4^+$ Treg and elevated $CD8^+$ IFNγ response (Supplementary Table S3). Even more dramatic benefits from monotherapy and combined treatment were noted for MC38 colon cancer ($P = 0.001$ between combination vs. anti-DC-HIL alone; **Fig. 4F** and **G**), with enhanced T-cell activation phenotype and decreased MDSC in tumor microenvironment (Supplementary Table S3). Thus, all three-tumor models are highly sensitive to both anti-PDL1 and anti-DC-HIL treatment.

We then examined effects of anti-PDL1 mAb on pre-established B16 melanoma metastasis in lung. Similarly, C57BL/6 mice were infused intravenously with B16 melanoma cells; 6 days later, all mice were treated with anti-DC-HIL or control IgG (200 μg/mouse) injected intraperitoneally (six injections total at different intervals of 2, 3, or 4 days). On day 18, we quantified the following metastasis indices: lung weight, number of foci, and melanin content per lung (**Fig. 5A**), while also measuring blood sDC-HIL. Anti-DC-HIL mAb reduced all

Published OnlineFirst December 10, 2019; DOI: 10.1158/1078-0432.CCR-19-2360

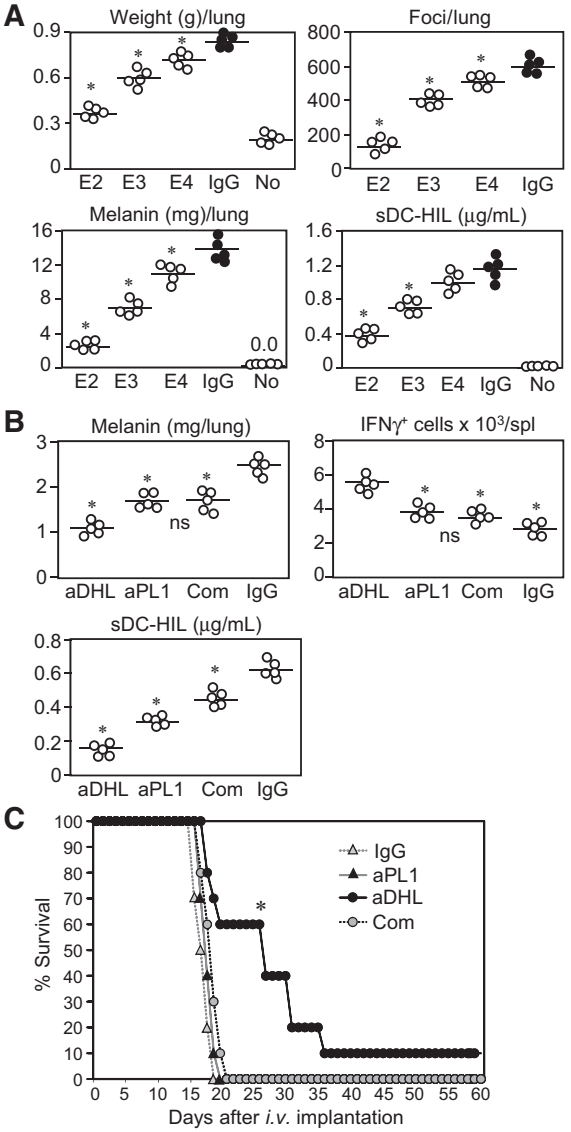

Figure 5.

B16 melanoma shows better response to anti-DC-HIL than anti-PDL1 treatment. **A,** Mice were injected intravenously with B16 melanoma cells; 6 days later mice were given intraperitoneal injection of anti-DC-HIL (aDHL) mAb or control IgG (200 μg/mouse) every 2 (E2), 3 (E3), or 4 days (E4). None (No) means tumor-free mice. Day 18, mice were scored for metastatic indices; lung weight, number of foci, melanin content, and blood sDC-HIL levels. **B,** Mice were similarly injected with B16 cells and treated with mAb every 2 days, and on day 18, mice were scored for melanin content and IFNγ-secreting cells per spleen. mAb includes anti-DC-HIL (the rabbit IgG V-region fused to mouse C-region), rat anti-PDL1, the combined mAb (Com), and mixture of rabbit and mouse control IgG (IgG). Mice were measured for metastasis indices. **C,** Kaplan–Meier plot; Day 0, mice ($n = 10$) were injected intravenously with B16 melanoma cells. Day 6, mice were given control Ab (IgG), anti-PDL1 (aPL1), anti-DC-HIL (aDHL), or combined (Com) mAb every 2 days until day 16, and every 3 days until day 28, and weekly injection. Survival rate (%) was monitored until day 60. $P = 0.0004$ between aDHL and other groups by Mantel–Cox test. *$P < 0.01$ compared with control. Ns, not significant. Data shown are representative of at least two independent experiments.

metrics in a dose-dependent manner, with the greatest effect noted for the most frequent treatment protocol every 2 days. We then compared the efficacy of anti-DC-HIL with anti-PDL1 mAb: B16 cells express the targets of both treatments (18). Anti-DC-HIL mAb markedly inhibited growth of B16 lung mets and increased the IFNγ response in draining lymph nodes ($P < 0.01$, **Fig. 5B**), whereas anti-PDL1 had a marginal effect. Surprisingly, combined treatment with both mAbs negated the benefit from anti-DC-HIL mAb (**Fig. 5B**). Antitumor activity of anti-DC-HIL mAb is most likely due to its ability to block interaction of DC-HIL with its ligand because the mAb cannot transduce the DC-HIL-specific intracellular signals (14) and because it blocks binding of DC-HIL to activated T cells (Supplementary Fig. S2).

We also examined effects of mAb treatment on survival rate of mice with B16 lung metastases (**Fig. 5C**). Tumor-bearing mice were treated as before, but this time the mAb treatments were sustained through 60 days. All control mice died by day 19 and all anti-PDL1–treated mice died by day 20. In contrast, 60% of anti-DC-HIL–treated mice remained alive, surviving through day 35 ($P = 0.0004$), with the exception of 1 mouse surviving by day 60. Similar results were noted in a repeat experiment. The longest surviving DC-HIL–treated mouse with melanoma appeared to develop memory T-cell response to B16 melanoma (Supplementary Fig. S3). Thus, B16 melanoma offers the great opportunity to study the role of DC-HIL molecules in suppressing response to ICI treatment.

Anti-DC-HIL treatment shifted lung mets toward a more immune competent milieu

We next examined the immune status of lung mets during the course of ICI therapy (over 14 days). Reproducibly, anti-PDL1 treatment decreased by 40% of blood sDC-HIL levels on day 14, whereas anti-DC-HIL did by 80% (Supplementary Fig. S4A). $CD45^+$ TIL were isolated from B16 lung mets and analyzed for frequency of immune cell subsets (Supplementary Fig. S4B). In control and treated mice, TIL were increased on day 7, followed by a reduction on day 14. Control mice showed the progressive increase in CD4 and CD8 T cells within TIL. Anti-DC-HIL mAb led to a greater increase over control in percentage of CD4 and CD8 T cells and percentage of $SD4^+$ and $PD1^+$ subsets and in their IFNγ responses. Anti-PDL1 mAb also produced rises in T cells and IFNγ responses but to a lesser degree compared with anti-DC-HIL mAb treatment. Combined treatment had no added value over monotherapy. With respect to MDSC, in control mice percent $CD11b^+Gr1^+$ MDSC in TIL was unchanged through 14 days, but there was a marked increase in the number of MDSC per gram of lung (Supplementary Fig. S4). Interestingly, DC-HIL^+MDSC subset expanded rapidly from 0.2% on day 0 to 45% on day 14, with hardly any MDSC expressing PDL1. Anti-DC-HIL mAb prevented MDSC expansion greater than did anti-PDL1 mAb, and combined treatment negated these effects. Thus, the two mAb appeared to compete with each other in their impact on the tumor microenvironment.

Host DC-HIL expression determines tumor response to anti-PDL1 treatment

Among tumor lines we used, B16 melanoma is unique in expressing DC-HIL (ref. 27; Supplementary Fig. S5). We thus examined whether tumor-DC-HIL expression accounts for resistance to anti-PDL1 therapy. We generated DC-HIL-knocked out (DC-$HIL^{-/-}$) B16 cells that do not express DC-HIL but retain high expression of PDL1. This engineered cell line had extensive *in vitro* growth ability, but with significantly slower *in vivo* tumor growth ability than parental B16 cells (18). Using this cell line, we examined influence of tumor-DC-HIL to anti-PDL1 response (**Fig. 6A**). DC-$HIL^{-/-}$ B16 cells showed as

Published OnlineFirst December 10, 2019; DOI: 10.1158/1078-0432.CCR-19-2360

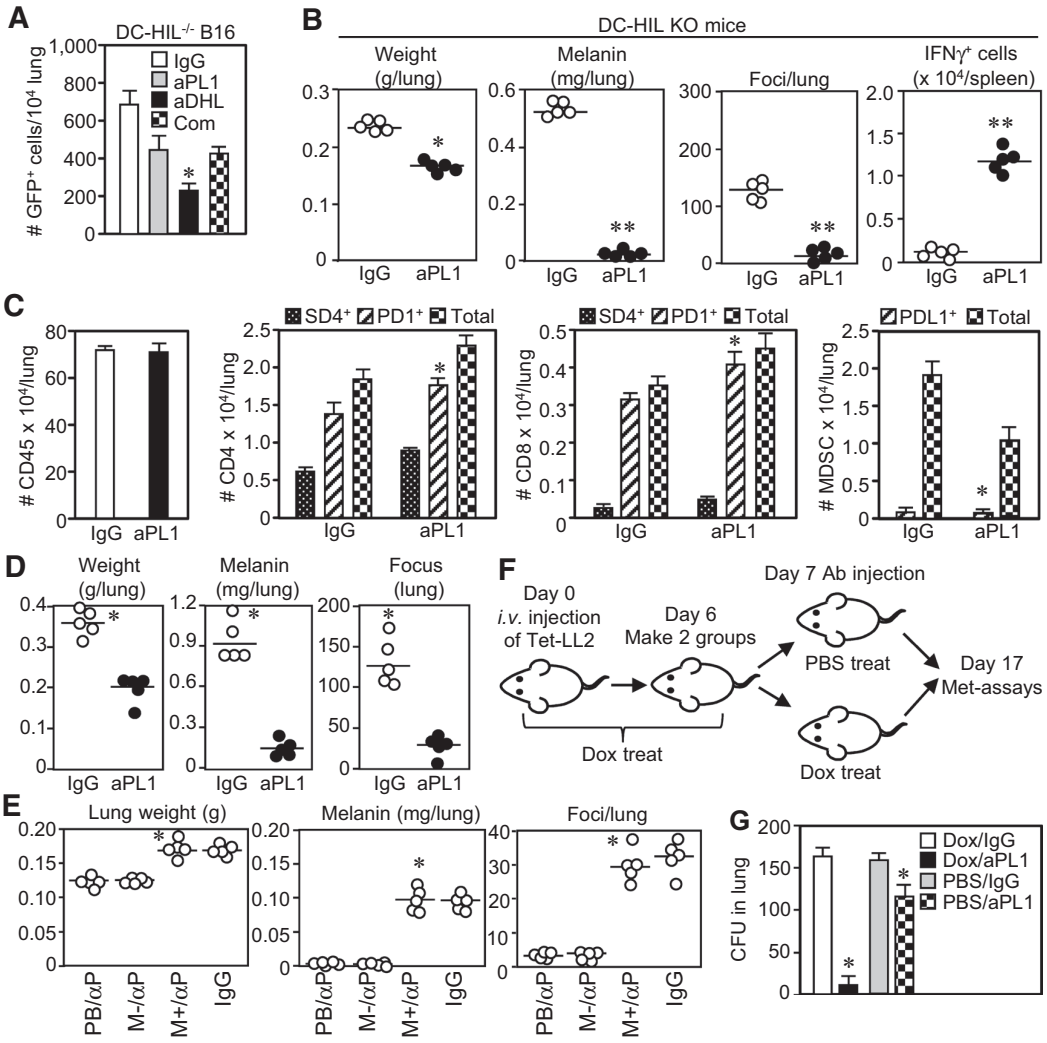

Figure 6.

Expression of host-derived DC-HIL determines tumor response to anti-PDL1. **A,** Mice bearing lung-metastatic GFP$^+$ DC-HIL$^{-/-}$B16 cells were similarly treated with control IgG (IgG), anti-PDL1 (aPL1), anti-DC-HIL (aDHL), or combination (Com), and tumor growth was quantified by number of GFP$^+$ cells among 10,000 lung cells. **B** and **C,** DC-HIL$^{-/-}$ mice with B16 lung mets were treated with control IgG or anti-PDL1 mAb. Lung metastasis was quantified for indicated indices (**B**) and lung cells were prepared and determined by flow cytometry for number of CD45$^+$ leukocytes, CD4$^+$, or CD8$^+$ T cells (SD4$^+$, PD1$^+$ subset, or total cells) per total lung (**C**). **D,** BM chimeric mice with transplantation of BM cells of DC-HIL$^{-/-}$ mice were injected intravenously with B16 cells and treated with IgG or mAb, followed by scoring metastasis. **E,** DC-HIL$^{-/-}$ mice with B16 lung mets were given intravenous injection of PBS (PB), DC-HIL^{neg} (M−), or DC-HIL$^+$MDSC (M+) and then treated with anti-PDL1 mAb (αP). IgG group was treated just with control IgG. After five injections, mice were quantified for metastasis indices. **F** and **G,** LL2-neo cells with Tet-Off-controlled sDC-HIL gene were injected intravenously into mice treated with Dox. On day 6, all mice were sorted into two groups, treated with Dox or PBS, followed by intraperitoneal injection of anti-PDL1 mAb or control IgG (**F**). On day 17, mice were quantified for metastasis by counting CFU of G418-resistant colonies and expressed as CFU in 1×10^6 lung cells (**G**). * and ** $P < 0.05$ and $P < 0.0001$, respectively, compared with control. Data shown are representative of at least two independent experiments.

a poor response to anti-PDL1 as did the parental cells, indicating that tumor-DC-HIL has no influence to this resistance. We next addressed whether host DC-HIL affects anti-PDL1 response (**Fig. 6B**). DC-HIL$^{-/-}$ mice bearing B16 lung metastases were treated with anti-PDL1 or control IgG. Anti-PDL1 treatment led to a remarkable decrease in all metastasis indices in DC-HIL$^{-/-}$ mice, including lung weight (0.23–0.18 g), melanin content (0.53–0.03 mg), and number of foci (127–14), with a 10-fold increase in IFNγ response. Although there was no difference in CD45$^+$ TIL number between anti-PDL1 and control treatments, anti-PDL1 mAb increased total CD4 and CD8 T cells and their SD4$^+$ and PD1$^+$ subsets, while decreasing total MDSC in the lung (**Fig. 6C**; Supplementary Fig. S6).

Because DC-HIL is also expressed by nonhematopoietic cells, we dissected influence of hematopoietic cell- versus nonhematopoietic cell-derived DC-HIL to anti-PDL1 response. We generated BM-chimeric mice, in which hematopoietic cells are originated from transplanted BM cells of DC-HIL$^{-/-}$ mice. Deletion of *DC-HIL* gene from hematopoietic cells (while nonhematopoietic DC-HIL

Published OnlineFirst December 10, 2019; DOI: 10.1158/1078-0432.CCR-19-2360

expression remains) failed to reverse the high response to anti-PDL1 (**Fig. 6D**), indicating that DC-HIL on nonhematopoietic cells is dispensable for B16 melanoma resistance to anti-PDL1 treatment.

Because melanoma-bearing hosts express DC-HIL as the receptor on MDSC and the soluble form (sDC-HIL), we addressed which molecular form is more important in regulating tumor responsiveness to anti-PDL1 mAb. For the impact of DC-HIL receptor, we examined whether adoptive transfer of DC-HIL^{+} MDSC into DC-HIL$^{-/-}$ mice bearing B16 lung mets reverses anti-PDL1 tumor response (**Fig. 6E**; Supplementary Fig. S7A). As control, DC-HIL^{neg} MDSC were also transferred into the host. Reproducibly, anti-PDL1 inhibited growth of B16 lung mets almost completely in DC-HIL$^{-/-}$ mice. This antitumor activity was diminished markedly by infusion of DC-HIL^{+} MDSC, whereas injection of DC-HIL^{neg} MDSC had no effect. For sDC-HIL, we used LL2 cells (which do not express DC-HIL) transfected with Tet-Off-controlled sDC-HIL gene (**Fig. 6F**). Immediately after intravenous injection of the LL2 transfectant, mice were given Dox for 6 days and then sorted into two groups; one was continued with Dox and the other was discontinued. These groups were also treated with anti-PDL1 or control IgG and scored for metastasis indices on day 17. sDC-HIL remained very low through day 6 but quickly increased to 8.4 to 9.6 ng/mL after Dox discontinuation, and low sDC-HIL levels (1–1.4 ng/mL) were maintained in Dox-continued group that exhibited very high response to anti-PDL1 mAb compared with IgG-treated mice (**Fig. 6G**). In contrast, doxycycline-discontinued group (sDC-HIL expressed) had markedly reduced antitumor activity. This reduced response was associated with increased total MDSC or DC-HIL^{+} subset of lung metastases (Supplementary Fig. S7B). Furthermore, adoptive transfer of DC-HIL^{+} (but not DC-HIL^{neg}) MDSC into DC-HIL-KO mice bearing LL2 tumor markedly reversed the benefit of anti-PDL1 treatment (Supplementary Fig. S8). Thus, both DC-HIL^{+} MDSC and sDC-HIL converted tumor cells from an anti-PDL1-responsive to resistant tumor.

Discussion

Primary resistance to ICI therapy has been attributed to tumor-cell deficiency in PDL1 expression or in IFNγ signaling (and thus insensitivity to IFNγ killing) and/or host defects in mounting T-cell responses (32, 33). T-cell suppressors also play a pivotal role particularly in attenuating the tumor Ag-specific T cells restored by intervening the PD1 pathway (34, 35). We underscore the importance of this suppressor mechanism by finding the significant correlation of high blood sDC-HIL levels and poor response to ICI immunotherapy for patients with advanced NSCLC. Furthermore, our animal studies have shown the possible interaction of host-derived T-cell-inhibitory DC-HIL molecules with the restored T cells by anti-PDL1 mAb in B16 melanoma and LL2 lung cancer.

In tumor-bearing hosts, DC-HIL is expressed as a transmembrane protein on myeloid cells and as a soluble form (sDC-HIL) secreted into peripheral blood. Although both forms share common structures, they are not identical in function. We have previously identified MDSC as the most abundant myeloid-cell sector expressing DC-HIL receptor in B16 melanoma-bearing mice (26). Lung metastases of B16 melanoma (and other tumors) recruited DC-HIL^{+}MDSC subsets such that these cells comprised up to 45% of lung-TIL. Surprisingly, PDL1^{+}MDSC subset numbered very few among lung-TIL, despite the fact that it comprised approximately 30% among total MDSC in subcutaneous B16 melanoma and in spleen of tumor-bearing mice (26). We speculate that lung-infiltrating DC-HIL^{+}MDSC, which are unaffected by anti-PDL1 mAb and suppress the function of T cells revitalized by anti-PDL1 mAb.

Unlike the cellular DC-HIL receptor, binding of sDC-HIL to the ligand SD4 on T cells is incapable of transducing its inhibitory signals, suggesting that sDC-HIL interferes with binding of DC-HIL receptor to the ligand (36, 37). In disagreement with this functional property, soluble PDL1 (sPDL1) was reported to transmit its inhibitory signal through activated CD4^{+} T cells (38). Recently, we showed sDC-HIL to also bind to the surface of endothelial cells (EC) of blood vessels with higher avidity than to T cells (28). Intriguingly, sDC-HIL bound to the surface of EC prevents selectively transendothelial migration of T cells into cancer tissues (17, 28). These findings led us to hypothesize that blood sDC-HIL hampers recruitment of T cells into tumors, resulting in reduced tumor-CD8 density, a requisite for successful anti-PDL1 treatment (39).

Combining anti-DC-HIL with anti-PDL1 mAb produced synergistic outcomes for treatment of all tumors except B16 melanoma, in which the latter mAb neutralized the effect of anti-DC-HIL mAb. Because combination treatment led to elevated expression of sDC-HIL in the host, we presume that treatment of B16 melanoma cells with anti-PDL1 mAb upregulated sDC-HIL expression that saturated the Ag-binding capacity of anti-DC-HIL mAb.

Given high costs, potential toxicities, availability of alternative therapies, and limited predictive value of existing biomarkers, ICI therapy can benefit from the identification of new markers that more reliably discriminate between response and resistance. Tumor-PDL1 expression has been used to predict ICI response for many cancers, but the lack of a standard method to measure this marker has made it inconsistent at best (40). Furthermore, PDL1-negative tumors may still benefit from ICI, making clinicians reluctant to base clinical decisions on the result. sPDL1 and sPD1 are generated by alternative splicing and secreted by cancer cells into blood, but their prognostic ability suffers from contradictory findings: one study of adenocarcinomas correlated high blood levels with better prognosis (41), whereas other studies of diffuse large B-cell lymphoma, hepatocellular carcinoma, and lung cancer showed a converse outcome (42, 43). Tumor-infiltrating lymphocytes are a pre-existing barometer of the T-cell response within tumors; however, its value is rendered null in most cases because the cancer is already bereft of T cells. Genetic profiling of cancers (tumor mutation burden, tumor cell gene expression, and microsatellite instability) provides good biologic characterization but its predictive ability has yet to be established (44). These foregoing markers reflect properties intrinsic to the cancer. In contrast, TIL and peripheral blood markers like DC-HIL on MDSC and sDC-HIL echo the immune response (45). In addition, blood elements have the advantage of being readily assayed and in a repeated fashion during the course of treatment.

Gpnmb/DC-HIL has been studied as a treatment target for melanoma, triple-negative breast cancer (TNBC), and NSCLC. Gpnmb mRNA level within tumors correlated with poor prognosis for melanoma (46) and increased risk for relapse of TNBC (47). The NSCLC cell lines express Gpnmb and secrete the soluble form, which can promote tumor growth in immunocompromised mice (48). However, we failed to detect sDC-HIL in the culture supernatant of NSCLC cells expressing DC-HIL on the cell surface. Our study showed CD14 monocytes (including MDSC) to be the primary secretors of sDC-HIL, which is a predictive marker for response of patients with NSCLC to ICI.

In sum, DC-HIL offers the promise of useful predictive blood markers (receptor on MDSC and the soluble moiety sDC-HIL) that embody a real-time measure of the cancer's interaction with the

Published OnlineFirst December 10, 2019; DOI: 10.1158/1078-0432.CCR-19-2360

immune system. Because our animal studies suggest that the significance of elevated DC-HIL levels as a predictive marker is not limited to treatment of lung cancer with ICI, our insights may be applicable to other malignancies and their immunotherapy. Nevertheless, adequately designed large prospective studies are warranted to establish blood sDC-HIL as a predictive biomarker for immunotherapy.

Disclosure of Potential Conflicts of Interest

No potential conflicts of interest were disclosed.

Authors' Contributions

Conception and design: D.E. Gerber, K. Ariizumi
Development of methodology: J.-S. Chung, M. Kobayashi
Acquisition of data (provided animals, acquired and managed patients, provided facilities, etc.): J.-S. Chung, V. Ramani, M. Kobayashi, V. Popat
Analysis and interpretation of data (e.g., statistical analysis, biostatistics, computational analysis): J.-S. Chung, S. Zhang
Writing, review, and/or revision of the manuscript: J.-S. Chung, V. Popat, S. Zhang, P.D. Cruz, D.E. Gerber, K. Ariizumi
Administrative, technical, or material support (i.e., reporting or organizing data, constructing databases): F. Fattah
Study supervision: K. Ariizumi

Acknowledgments

We are grateful to Irene Dougherty for technical assistance and Rolf Brekken for NSCLC cell lines. This study was primarily supported by VA Merit Award (1I01BX004069) and Department of Defense Lung Cancer Research Program (W81XWH-18-1-0312) and also partially supported by American Cancer Society/Melanoma Research Alliance (132330-MRAT-18-114-01-LIB/597700), The University of Texas SPORE in Lung Cancer, and the Harold C. Simmons Comprehensive Cancer Center's Biomarker Research Core (1P30-CA142543–03).

The costs of publication of this article were defrayed in part by the payment of page charges. This article must therefore be hereby marked *advertisement* in accordance with 18 U.S.C. Section 1734 solely to indicate this fact.

Received July 22, 2019; revised November 7, 2019; accepted December 4, 2019; published first December 10, 2019.

References

1. Prabhu Das MR, Zamvil SS, Borriello F, Weiner HL, Sharpe AH, Kuchroo VK. Reciprocal expression of co-stimulatory molecules, B7-1 and B7-2, on murine T cells following activation. Eur J Immunol 1995;25:207–11.
2. Weber J. Immune checkpoint proteins: a new therapeutic paradigm for cancer–preclinical background: CTLA-4 and PD-1 blockade. Semin Oncol 2010;37:430–9.
3. Dong H, Strome SE, Salomao DR, Tamura H, Hirano F, Flies DB, et al. Tumor-associated B7-H1 promotes T-cell apoptosis: a potential mechanism of immune evasion. Nat Med 2002;8:793–800.
4. Lee L, Gupta M, Sahasranaman S. Immune checkpoint inhibitors: an introduction to the next generation cancer immunotherapy. J Clin Pharmacol 2015;56:157–69.
5. Bagley SJ, Bauml JM, Langer CJ. PD-1/PD-L1 immune checkpoint blockade in non-small cell lung cancer. Clin Adv Hematol Oncol 2015;13:676–83.
6. Topalian SL, Hodi FS, Brahmer JR, Gettinger SN, Smith DC, McDermott DF, et al. Safety, activity, and immune correlates of anti-PD-1 antibody in cancer. N Engl J Med 2012;366:2443–54.
7. Homet Moreno B, Parisi G, Robert L, Ribas A. Anti-PD-1 therapy in melanoma. Semin Oncol 2015;42:466–73.
8. Powles T, Eder JP, Fine GD, Braiteh FS, Loriot Y, Cruz C, et al. MPDL3280A (anti-PD-L1) treatment leads to clinical activity in metastatic bladder cancer. Nature 2014;515:558–62.
9. Massari F, Santoni M, Ciccarese C, Santini D, Alfieri S, Martignoni G, et al. PD-1 blockade therapy in renal cell carcinoma: current studies and future promises. Cancer Treat Rev 2015;41:114–21.
10. Sharma P, Hu-Lieskovan S, Wargo JA, Ribas A. Primary, adaptive, and acquired resistance to cancer immunotherapy. Cell 2017;168:707–23.
11. Kuan CT, Wakiya K, Dowell JM, Herndon JE II, Reardon DA, Graner MW, et al. Glycoprotein nonmetastatic melanoma protein B, a potential molecular therapeutic target in patients with glioblastoma multiforme. Clin Cancer Res 2006;12:1970–82.
12. Chung JS, Tomihari M, Tamura K, Kojima T, Cruz PD Jr, Ariizumi K. The DC-HIL ligand syndecan-4 is a negative regulator of T-cell allo-reactivity responsible for graft-versus-host disease. Immunology 2013;138:173–82.
13. Chung JS, Sato K, Dougherty II, Cruz PD Jr, Ariizumi K. DC-HIL is a negative regulator of T lymphocyte activation. Blood 2007;109:4320–7.
14. Chung JS, Yudate T, Tomihari M, Akiyoshi H, Cruz PD Jr, Ariizumi K. Binding of DC-HIL to dermatophytic fungi induces tyrosine phosphorylation and potentiates antigen presenting cell function. J Immunol 2009;183:5190–8.
15. Shikano S, Bonkobara M, Zukas PK, Ariizumi K. Molecular cloning of a dendritic cell-associated transmembrane protein, DC-HIL, that promotes RGD-dependent adhesion of endothelial cells through recognition of heparan sulfate proteoglycans. J Biol Chem 2001;276:8125–34.
16. Kobayashi M, Chung JS, Beg M, Arriaga Y, Verma U, Courtney K, et al. Blocking monocytic myeloid-derived suppressor cell function via anti-DC-HIL/GPNMB antibody restores the in vitro integrity of T cells from cancer patients. Clin Cancer Res 2019;25:828–38.
17. Rose AA, Annis MG, Dong Z, Pepin F, Hallett M, Park M, et al. ADAM10 releases a soluble form of the GPNMB/Osteoactivin extracellular domain with angiogenic properties. Plos One 2010;5:e12093.
18. Tomihari M, Chung JS, Akiyoshi H, Cruz PD Jr, Ariizumi K. DC-HIL/glycoprotein Nmb promotes growth of melanoma in mice by inhibiting the activation of tumor-reactive T cells. Cancer Res 2010;70:5778–87.
19. Pentcheva-Hoang T, Chen L, Pardoll DM, Allison JP. Programmed death-1 concentration at the immunological synapse is determined by ligand affinity and availability. Proc Natl Acad Sci U S A 2007;104:17765–70.
20. Chung JS, Cruz PD Jr, Ariizumi K. Inhibition of T-cell activation by syndecan-4 is mediated by CD148 through protein tyrosine phosphatase activity. Eur J Immunol 2011;41:1794–9.
21. Peng W, Liu C, Xu C, Lou Y, Chen J, Yang Y, et al. PD-1 blockade enhances T-cell migration to tumors by elevating IFN-gamma inducible chemokines. Cancer Res 2012;72:5209–18.
22. Khan S, Khan SA, Luo X, Fattah FJ, Saltarski J, Gloria-McCutchen Y, et al. Immune dysregulation in cancer patients developing immune-related adverse events. Br J Cancer 2019;120:63–8.
23. Davies M. New modalities of cancer treatment for NSCLC: focus on immunotherapy. Cancer Manag Res 2014;6:63–75.
24. Gerber DE, Urbanic JJ, Langer C, Hu C, Chang IF, Lu B, et al. Treatment design and rationale for a randomized trial of cisplatin and etoposide plus thoracic radiotherapy followed by nivolumab or placebo for locally advanced non-small-cell lung cancer (RTOG 3505). Clin Lung Cancer 2017;18:333–9.
25. Eisenhauer EA, Therasse P, Bogaerts J, Schwartz LH, Sargent D, Ford R, et al. New response evaluation criteria in solid tumours: revised RECIST guideline (version 1.1). Eur J Cancer 2009;45:228–47.
26. Chung JS, Tamura K, Cruz PD Jr, Ariizumi K. DC-HIL-expressing myelomonocytic cells are critical promoters of melanoma growth. J Invest Dermatol 2014;1342784–94.
27. Ramani V, Teshima T, Tamura K, Chung JS, Kobayashi M, Cruz PD Jr, et al. Melanoma-derived soluble DC-HIL/GPNMB promotes metastasis by excluding T-lymphocytes from the pre-metastatic niches. J Invest Dermatol 2018;138:2443–51.
28. Anderegg U, Eichenberg T, Parthaune T, Haiduk C, Saalbach A, Milkova L, et al. ADAM10 is the constitutive functional sheddase of CD44 in human melanoma cells. J Invest Dermatol 2009;129:1471–82.
29. Singhal S, Miller D, Ramalingam S, Sun SY. Gene expression profiling of non-small cell lung cancer. Lung cancer 2008;60:313–24.
30. Shingyoji M, Ando S, Nishimura H, Nakajima T, Ishikawa A, Itakura M, et al. VEGF in patients with non-small cell lung cancer during combination chemotherapy of carboplatin and paclitaxel. Anticancer Res 2009;29:2635–9.

31. Zimmerman M, Hu X, Liu K. Experimental metastasis and CTL adoptive transfer immunotherapy mouse model. J Vis Exp 2010(45):pii. 2077.
32. Shukuya T, Carbone DP.Predictive markers for the efficacy of anti-PD-1/PD-L1 antibodies in lung cancer. J Thorac Oncol 2016;11:976–88.
33. Benci JL, Xu B, Qiu Y, Wu TJ, Dada H, Twyman-Saint Victor C, et al. Tumor interferon signaling regulates a multigenic resistance program to immune checkpoint blockade. Cell 2016;167:1540–54.
34. Lindau D, Gielen P, Kroesen M, Wesseling P, Adema GJ. The immunosuppressive tumour network: myeloid-derived suppressor cells, regulatory T cells and natural killer T cells. Immunology 2013;138:105–15.
35. Frey AB.Myeloid suppressor cells regulate the adaptive immune response to cancer. J Clin Invest 2006;116:2587–90.
36. Chung JS, Dougherty I, Cruz PD Jr, Ariizumi K. Syndecan-4 mediates the coinhibitory function of DC-HIL on T cell activation. J Immunol 2007;179: 5778–84.
37. Chung JS, Bonkobara M, Tomihari M, Cruz PD Jr, Ariizumi K. The DC-HIL/syndecan-4 pathway inhibits human allogeneic T-cell responses. Eur J Immunol 2009;39:2009.
38. Zhou J, Mahoney KM, Giobbie-Hurder A, Zhao F, Lee S, Liao X, et al. Soluble PD-L1 as a biomarker in malignant melanoma treated with checkpoint blockade. Cancer Immunol Res 2017;5:480–92.
39. Uryvaev A, Passhak M, Hershkovits D, Sabo E, Bar-Sela G. The role of tumor-infiltrating lymphocytes (TILs) as a predictive biomarker of response to anti-PD1 therapy in patients with metastatic non-small cell lung cancer or metastatic melanoma. Med Oncol 2018;35:25.
40. Patel SP, Kurzrock R.PD-L1 expression as a predictive biomarker in cancer immunotherapy. Mol Cancer Ther 2015;14:847–56.
41. Zheng Z, Bu Z, Liu X, Zhang L, Li Z, Wu A, et al. Level of circulating PD-L1 expression in patients with advanced gastric cancer and its clinical implications. Chinese J Cancer Res 2014;26:104–11.
42. Rossille D, Gressier M, Damotte D, Maucort-Boulch D, Pangault C, Semana G, et al. High level of soluble programmed cell death ligand 1 in blood impacts overall survival in aggressive diffuse large B-cell lymphoma: results from a French multicenter clinical trial. Leukemia 2014;28:2367–75.
43. Finkelmeier F, Canli O, Tal A, Pleli T, Trojan J, Schmidt M, et al. High levels of the soluble programmed death-ligand (sPD-L1) identify hepatocellular carcinoma patients with a poor prognosis. Eur J Cancer 2016;59:152–9.
44. Chan TA, Yarchoan M, Jaffee E, Swanton C, Quezada SA, Stenzinger A, et al. Development of tumor mutation burden as an immunotherapy biomarker: utility for the oncology clinic. Ann Oncol 2019;30:44–56.
45. Tong M, Wang J, He W, Wang Y, Pan H, Li D, et al. Predictive biomarkers for tumor immune checkpoint blockade. Cancer Manag Res 2018;10:4501–7.
46. Taya M, Hammes SR. Glycoprotein non-metastatic melanoma protein B (GPNMB) and cancer: a novel potential therapeutic target. Steroids 2017;133: 102–7.
47. Rose AA, Grosset AA, Dong Z, Russo C, Macdonald PA, Bertos NR, et al. Glycoprotein nonmetastatic B is an independent prognostic indicator of recurrence and a novel therapeutic target in breast cancer. Clin Cancer Res 2010;16: 2147–56.
48. Oyewumi MO, Manickavasagam D, Novak K, Wehrung D, Paulic N, Moussa FM, et al. Osteoactivin (GPNMB) ectodomain protein promotes growth and invasive behavior of human lung cancer cells. Oncotarget 2016; 7:13932–44.

Published OnlineFirst December 10, 2019; DOI: 10.1158/1078-0432.CCR-19-2360

AACR American Association for Cancer Research

Clinical Cancer Research

DC-HIL/Gpnmb Is a Negative Regulator of Tumor Response to Immune Checkpoint Inhibitors

Jin-Sung Chung, Vijay Ramani, Masato Kobayashi, et al.

Clin Cancer Res 2020;26:1449-1459. Published OnlineFirst December 10, 2019.